EMTP Tech Notes

for users of the Electromagnetic Transients Program

Issue # 94-2 ***April, 1994*** ***Editor: Thomas Grebe***

in this issue:

Letter from the Editor:

EMTP Tech Notes is the technical newsletter provided to members of the EMTP User's Group. The newsletter is a quarterly technical publication highlighting contributions from members of the User's Group. This newsletter is published using Microsoft Word for Windows 6.0. If you wish to contribute an article, please contact Susie Brockman or myself for appropriate text and figure formats. Contributions in the following areas are welcome:

- Technical articles
- Modifications / enhancements to the code
- Case studies / unique simulations
- Research projects
- EMTP data preparation / model development
- Modules developed for distribution on the BBS
- Letters to the editor / User's Group
- Technical paper abstracts
- Questions for members of the User's Group

I believe that the exchange of technical information is one of the most important functions of the EMTP User's Group and this newsletter will help to serve the needs of the members. Thanks to the authors for helping to put this issue together. As always, I'm open for suggestions regarding this publication and the User's Group in general.

Thanks for your support

For more information concerning the newsletter or to submit a contribution please contact:

Thomas Grebe (x33) or Susie Brockman (x41)
EMTP User's Group
Electrotek Concepts, Inc.
10305 Dutchtown Road, Suite 103
Knoxville, Tennessee 37932
Phone: (615) 675-1500 x33
FAX: (615) 966-5497

(800) 554-4767

ASD Nuisance Tripping

Applying a User's Group Model - An End-User's Perspective

This article documents the experience of one user in applying a User's Group supplied model to evaluate the effects of voltage magnification during capacitor switching as it relates to ASD tripping. The purpose of this paper is to let other end-users see how an existing model was applied and to let model developer's glimpse at how their finished product is used.

Introduction

The duties which many of you perform daily are typical of those I also do as a System Planner for a utility. For this reason, I felt it would be of benefit to share an experience in applying a "canned" Electromagnetic Transient Program (EMTP) model to an everyday situation. Over time, as an EMTP user, you have probably created your own models to solve a given problem. This is not done all the time because we all find it easier to "piece together" a data file from those we have used in the past, from those we have collected from friends and colleagues, and, more recently, from the EMTP User's Group. This last option is accessible via the Bulletin Board, User's Group meetings, Tech Notes, and the EMTP Case Study Workbook[1]. I have found this convenient for several reasons. First, I don't have the time to develop models for all the situations that I must deal with each day. Second, I don't always have the technical ability to build a model, even if time was not a problem. It takes an in-depth knowledge of specific equipment to build a model that "accurately" reveals that equipment's operation. If we are honest with ourselves, most of us would have to agree with these two observations. From this background, I would like to take us through a typical problem and it's solution using a Case Study Workbook Book data file, NUISANCE.DAT.

The Problem

We were approached by an industrial customer seeking service for a proposed plant, whose load would consist mainly of ASDs. This customer was seeking a site that would be capable of supplying their electrical needs with a minimum of interruptions. Due to the nature of their operation, even short duration interruptions would have the potential of tripping their ASDs and causing a disruption of their production that could last up to 4 DAYS. For this reason, each proposed plant site would have to evaluate all possible conditions that might cause an outage of their equipment and provide a "best guess" as to it's probability. This in effect was creating a "reliability factor" for each site. Sufficient information was provided on their equipment so that it's limitations could be determined. Such things as breaker operations, lightning strikes, line switching, existing equipment operation and starting, and capacitor switching were investigated. Ultimately, harmonics were also investigated, using SuperHarm. The remainder of this paper will focus on using an EMTP model to determine if capacitor switching will cause their ASDs to trip and, if so, examine the effect of possible remedies.

Data Collection and Model Building

Before building the model, the data requirements must be understood and the appropriate data collected. To help in this process, I first ran NUISANCE.DAT as-is to examine it's output and familiarize myself with the data it used. This also helped in understanding the mechanics of the model. The next step was to determine what others had done to investigate this problem. The first place for anyone to start is the EMTP Case Study Workbook itself. It carries you through the use of the model, showing how the data file is built. It also contains, in Appendix A , four articles that address the issue[2][3][4][5]. They expand on the building of the model and also explain the ramifications of varying various system parameters. These discussions should be used as a guide to determine which system variables you should investigate changing. They also serve as a guide for asking an equipment vendor for the appropriate data that fits your particular case.

The data needs of the model can be broken into two basic areas, the system components and the ASD drive components. All of the system data should be available to the utility engineer, since the majority represents the utility system. There is a small portion representing the customer's system to the point of connection to the ASD, which the customer should provide. Non-utility engineers performing this study would need to acquire the appropriate system model or equivalent from the serving utility. The EMTP Case Study Workbook details the converting of this data to the format usable by EMTP and the Rule Book[6] is also handy. The effort taken to insure the accuracy of the system data will be rewarded in the accuracy of the outcome. The system modeled in our case is shown in Figure 1. For brevity, only one scenario is shown and discussed but the principal is the same for all. Enough of the system should be modeled to insure that the proper reaction can be experienced.

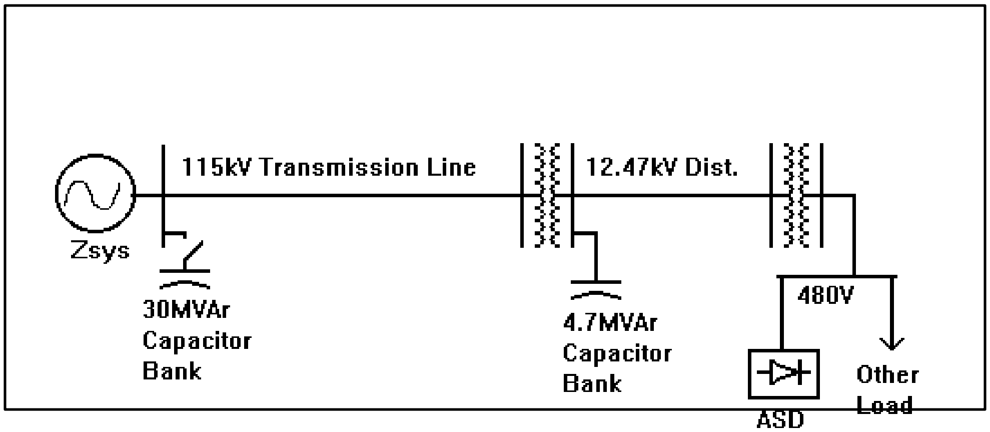

Figure 1 - System Single-Line Diagram

The ASD model in the data file is comprised of TACS data and circuit data. It is this portion of an EMTP data file that most of us rely on someone else to develop and leave for us to use. A model can best be used, however, the more it's inner workings are understand. As Tom Grebe has urged us, the best place to find at least a grounding in this subject is a good power electronics textbook such as [7], which we should at sometime have in our possession. Using it we can learn the "method of their madness" and, if nothing else, earn a greater appreciation for those that developed the model. In Figure 2, I have reproduced the data parameters needed for the ASD, as shown in [5], page 2.

Drive Data:

dc link capacitor size = 12,500uF
Drive output frequency = 45Hz
PWM switching frequency = 675Hz
Frequency modulation ratio (m_f) = 15
Amplitude modulation ratio (m_a) = 1.0

Motor Data:

Induction motor rating = 25HP
Efficiency = 85%
Power factor = 87%
Slip = 2.5%
X_s+X_r = 16%
X_m = 250%
$R_s = R_r$ = 5%

Figure 2 - Typical ASD data

Also to understand the model, it is helpful for us to have a visual picture of the drive itself. This I have also borrowed from [5], page 2, Figure 1, and included here as Figure 3. To prepare our model for use, we must take the manufacturer's data and place it in the proper format. This is done by examining the Case Study Workbook data file. Let us first look at a portion of the model in the data file, shown in Figure 4.

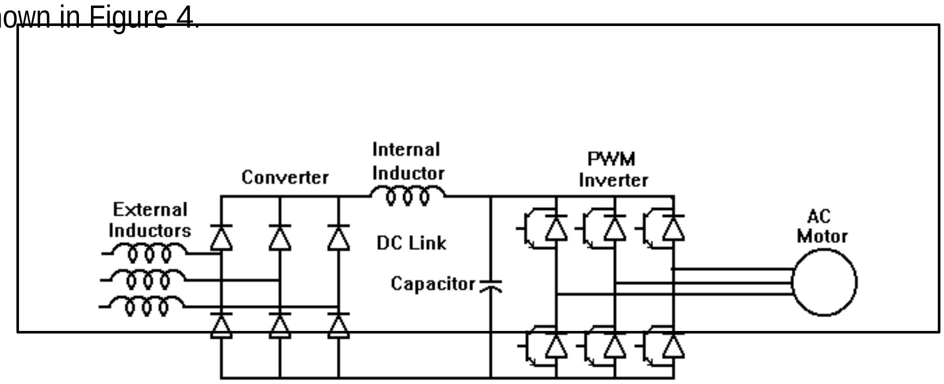

Figure 3 - ASD Single-line

```
/TACS
C
C <-------- Drive (Motor Speed) Frequency DF = 45 Hz
C
C Name->xx=<---------Fortran Expression--------------------------
98DF      =   45.00
C .....^xx=...........................
C
C <-------- Amplitude Modulation Ratio  = 1.00
C
C Name->xx=<---------Fortran Expression--------------------------
98MA      =   1.00
C .....^xx=...........................
C
C <-------- PWM Switching frequency FS = 675 Hz, (Mf = 675/45=15)
C
C Name->xx=<---------Fortran Expression--------------------------
98FS      =  675.00
C .....^xx=...........................
C
C <-------- Triangular voltage "VTRI" (next 5 cards)
C
C Name->xx<-----Ampl<---T(sec)<-Wid(sec)<------------------><---Tstart<----Tstop
23PULS            2.0 1.481E-3 0.7407E-3                      372.0E-6
C .....^xx.........^.........^.........^xxxxxxxxxxxxxxxxxxxx.........^.........^
C
```

Figure 4 -ASD TACS Data

Notice that the model requires data concerning the speed and frequency of the drive. Simply insert the data provided by the vendor into the appropriate place. Note that the Drive Output Frequency times the Frequency Modulation Ratio equals the PWM Switching Frequency. Also note that the Triangular Voltage (VTRI) card, a TACS pulse source, uses a time between pulses, T(sec), of 1.481E-3 sec's., which is 1/(PWM Switching Frequency) or 1/675. The pulse width, Wid(sec.), is 1/(2*675) and the start time, Tstart, is 1/(4*675). These ratio's were "backwards" derived but they seem to work. Toward the end of the data file, as shown on Figure 5, is another portion where the drive data must be entered.

```
/SOURCE
C
C <-------- Back EMF Voltage
C
C Bus-->xx<-----Ampl<-----Freq<----Phase<------------------><---Tstart<----Tstop
14MOTORA     230.380    45.000    -6.100                      26.0E-06     9999.
C .....^xx.........^.........^.........^xxxxxxxxxxxxxxxxxxxx.........^.........^
C
C Busl->xx<----Ratio<-Busk<-Busm<-Busx
18MOTORX         0.0            MONITA
C .....^xx.........^.....^.....^.....^
C
C Bus-->xx<-----Ampl<-----Freq<----Phase<------------------><---Tstart<----Tstop
14MOTORB     230.380    45.000    -126.1                      26.0E-06     9999.
C .....^xx.........^.........^.........^xxxxxxxxxxxxxxxxxxxx.........^.........^
C
C Busl->xx<----Ratio<-Busk<-Busm<-Busx
18MOTORY         0.0            MONITB
C .....^xx.........^.....^.....^.....^
C
C Bus-->xx<-----Ampl<-----Freq<----Phase<------------------><---Tstart<----Tstop
14MOTORC     230.380    45.000     113.9                      26.0E-06     9999.
C .....^xx.........^.........^.........^xxxxxxxxxxxxxxxxxxxx.........^.........^
C
C Busl->xx<----Ratio<-Busk<-Busm<-Busx
18MOTORZ         0.0            MONITC
C .....^xx.........^.....^.....^.....^
C
```

Figure 5 - ASD Motor Model

In this section, the Freq. is the Drive Output Frequency as given by the vendor. The reason for the other values is not known so their value was left as in the original file. Just above the file portion shown in Figure 5, we find the section reproduced as Figure 6.

```
/BRANCH
C
C <-------- Thevenin Equivalent Impedance
C           [ 3-phase, 60Hz, 4 pole, 460 V, 10HP Induction Motor - @ 45 Hz)
C
C <---Nodes--><---Refer--><-ohms<---mH<---uF<--------------------------------Out
C <-Bus1<-Bus2<-Bus3<-Bus4<----R<----L<----C                                  V
  PWMV_AMOTORA               3.0 13.26
  PWMV_BMOTORB               3.0 13.26     This should be V2/kVA , 1/3 per phase
  PWMV_CMOTORC               3.0 13.26
C .....^.....^.....^.....^.....^.....^.....^..................................^
C
```

Figure 6 - Motor Equivalent

This section details the drive motor size, which in our case was 10HP as shown. The ohms and mH can be calculated from the motor HP, operating voltage, PF, and eff. for any other given motor size. The values supplied with the original file yield 12.1kVA @ .51PF, if you work backwards to arrive at their input, not the expected 10kVA @ .87PF. Next, we must adjust the data in the DC link to match our situation. The modified section is shown in Figure 7.

```
/BRANCH
C
C <-------- dc Bus Components (12500uF capacitor)
C
C <---Nodes--><---Refer--><-ohms<---mH<---uF<--------------------------------Out
C <-Bus1<-Bus2<-Bus3<-Bus4<----R<----L<----C                                  V
  STARTRDCPLUS             0.001  0.01         DC link inductor               1
C .....^.....^.....^.....^.....^.....^.....^..................................^
  DCMNUSDCPLUS            10000.               DC load, if motor not modeled
C .....^.....^.....^.....^.....^.....^.....^..................................^
  DCPLUSDCMNUS                        12500.   DC link capacitor              2
C .....^.....^.....^.....^.....^.....^.....^..................................^
  RECPOS                                 1.0
C .....^.....^.....^.....^.....^.....^.....^..................................^
  RECNEG                                 1.0
C .....^.....^.....^.....^.....^.....^.....^..................................^
  RECNEGDCMNUS             0.001  0.01
C .....^.....^.....^.....^.....^.....^.....^..................................^
C
```

Figure 7 - DC Link Values

In this data section, the appropriate vendor's supplied data must be entered to correctly model the DC link. The vendor supplied capacitor value to be used must be entered. Vendors can install an inductor in the DC link to improve operation during transient conditions. External inductors can also be installed in front of the entire drive, but it would require three. In many situations, where a problem is to be fixed after the drive has been installed, it is easiest to place external inductors in front of the drive. In our case, the vendor was supplying new drives to the customer and would factory install the internal inductor. For an initial run, we will leave the value of the internal inductor as 0.01. The DC load can be modeled as a resistance value in this section if it is not desired to have a detailed model of the PWM inverter and the induction motor. If a more complete model is used, as in our case, this DC load value should be a large value. The final step is to model the external inductors as shown in Figure 8.

```
C
C <-------- Choke (Input) Impedance (0%)
C
C <---Nodes--><----------><-----------Ohms<-------------mH<-------------uF<-Out¿
C Bus1->Bus2-><----------><-------------R<-------------L<--------------C     V
  CHOKEATRMNLA                         0.001            0.01                  1
  CHOKEBTRMNLB                         0.001            0.01  External inductors
  CHOKECTRMNLC                         0.001            0.01
C .....^.....^xxxxxxxxxxxx..............^..............^..............^xxxxx^
C
```

Figure 8 - External Inductor Values

I found that the supplied inductor values, which simulate no external inductors, will solve but the output does not represent reasonable results. As shown in Figure 9., the voltage wave forms are greatly distorted. To obtain reasonable results, when modeling no external inductors, it was necessary to make the external inductor value at least 0.2% on the motor base, in this case 10HP. My section of the input inductor data looks like Figure 10.

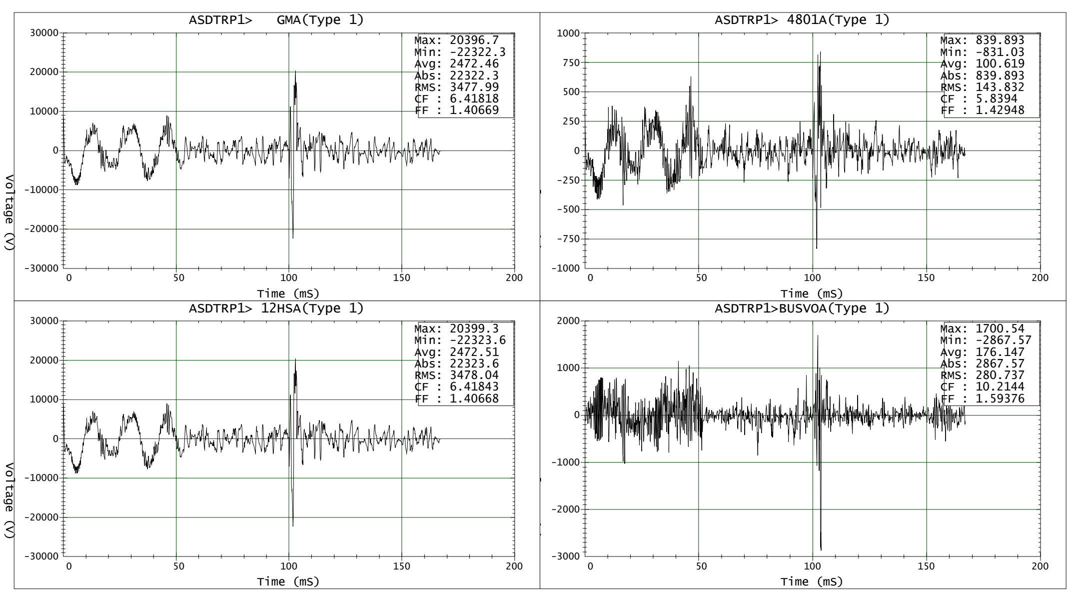

Figure 9 - Voltage Wave forms - Minimum Inductance

```
C
C <-------- Choke (Input) Impedance (0.2%)
C
C <---Nodes--><----------><-----------Ohms<-------------mH<-------------uF<-Out¿
C Bus1->Bus2-><----------><-------------R<-------------L<--------------C     V
  CHOKEATRMNLA                      0.001        0.12223                     1
  CHOKEBTRMNLB                      0.001        0.12223  External inductors
  CHOKECTRMNLC                      0.001        0.12223
C .....^.....^xxxxxxxxxxxx..............^..............^..............^xxxxx^
```

Figure 10 - 0.2% External Inductor Values

A solution using these values yields output voltages as shown in Figure 11, which are more reasonable. This and the previous display, Figure 9, was run while disabling the capacitor switching. This now completes the building of our data file with our model of the ASD, using the vendor supplied data, included. In this article, the actual vendor data is not used as it is proprietary, but the principal is the same.

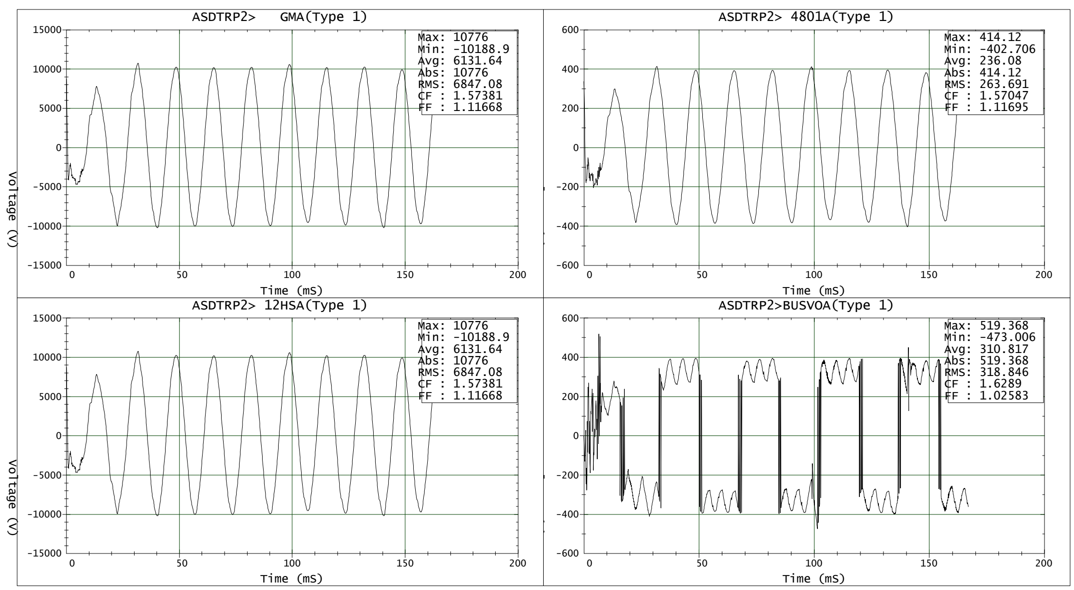

Figure 11 - Voltage Wave forms - 0.2% Inductor

As an exercise after the fact, data files were built that used two additional methods of modeling the ASD. The first set utilized a simplified model where the PWM inverter and drive motor was modeled as a resistance in the DC link. This was alluded to earlier and shown below as Figure 12. This method was also discussed at the Oct. 93 User's Group meeting in Dallas and detailed in the

Case Study Workbook from that meeting [8],pages 98-99, and distributed as 3PDIODE.DAT.

```
/BRANCH
C
C <-------- dc Bus Components (12500uF capacitor)
C
C <---Nodes--><---Refer--><-ohms<---mH<---uF<-------------------------------Out
C <-Bus1<-Bus2<-Bus3<-Bus4<----R<----L<----C                                  V
  STARTRDCPLUS             0.001  0.01         DC link inductor               1
C .....^.....^.....^.....^.....^.....^.....^..................................^
  DCMNUSDCPLUS             41.99               DC load, 10HP motor
C .....^.....^.....^.....^.....^.....^.....^..................................^
  DCPLUSDCMNUS                          12500.   DC link capacitor            2
C .....^.....^.....^.....^.....^.....^.....^..................................^
  RECPOS                                  1.0
C .....^.....^.....^.....^.....^.....^.....^..................................^
  RECNEG                                  1.0
C .....^.....^.....^.....^.....^.....^.....^..................................^
  RECNEGDCMNUS             0.001  0.01
C .....^.....^.....^.....^.....^.....^.....^..................................^
C
```

Figure 12 - Simplified Model DC Link

The 41.99 ohms represents a 10HP motor and the previous motor model, which is all the data following the Diodes (front-end) down to the line prior to Output Request may be deleted, as shown in Figure 13 below.

```
/SWITCH
C
C <-------- Diodes (front-end)
C
C BUS-->BUS--><------Vig<----Ihold<-------td<---------CLOSEDSame<Grid<Op/Cl<xxOO
11DIOD1ADIOD1C               0.1
11DIOD3ADIOD3C               0.1
11DIOD5ADIOD5C               0.1
C .....^.....^.........^.........^.........^xxxxxxxxxx^.....^...^.....^.....^xx^^
11DIOD4ADIOD4C               0.1
11DIOD6ADIOD6C               0.1
11DIOD2ADIOD2C               0.1
C .....^.....^.........^.........^.........^xxxxxxxxxx^.....^...^.....^.....^xx^^
C
C
C <-------------------------------------------------Branch Data-----------------
C
                  Delete all data between these two lines
C
C <-------------------------------------------------Output Request---------------
C
```

Figure 13 - Diode Front End

File Section to be Deleted

The next model investigated is an expanded one, which again is based on material presented at the October User's Group meeting and appearing in it's report [8], pages 85-87. The Case Study Workbook [1] also contains information on this model in Section 3 and it's included file PWMMOTOR.DAT. This model utilizes a U. M. induction motor model and input data provided in Figure 2 is used. Some of the motor data may not always be easily obtained from your customer and/or his vendor. Again, use Figure 13 above to remove the original motor model from your file. Then, using PWMMOTOR.DAT, cut out the file section between the above marked areas and insert it into your working file. This inserted portion will have to be modified as shown in Figure 14 below. [8], page 88 and [6], section 10.12, can be used to obtain the appropriate formulas.

```
C <-------- Adjustable Current Source for Torque Compensation
C
C --Bus><><-----Ampl<-----Freq<----Phase<-------A1<------T1><---Tstart<----Tstop
14ADJUST-1 -0.000001   0.00001                                -1.00E-3      9999
C .....^.^.........^.........^.........^.........^........^..........^.........^
14LDTORQ-1  -40.5900   0.00001                                150.0E-3      9999
C .....^.^.........^.........^.........^.........^........^..........^.........^
C
C  Torque = (10HP * 746kW/HP) / [(1-0.025) * 188.5rad/sec] = 40.59 N-M
C
C
C <-------- Machine Data (5-25 HP data parameters)
C
C  3-phase, 4-pole, 60 Hz, 480 V (line-to-line)
C  Efficiency = 0.87, power factor = 0.85, full load slip = 2.5%
C  Xs=Xr = 0.16 pu, Xm = 2.5 pu, Rs=Rr = 0.05 pu
C
C Class 1 U.M. Data Cards
C card (1) indicates the request for the use of a U.M. model (19 - col 1-2)
C <------------------------------------------------------------------------------
19
C card (2) general specification
C (with SI unit and residual magnetism option - 2 in col 1,
C request automatic steady-state initialization - 1 in col 2,
C compensation is used for interfacing U.M. with the external electric network)
C <-----------<------------------------------------------------------------------
21            0
C xxxxxxxxxxxx^ (INPU - col 1, INITUM - col 2, ICOMP - col 15)
C
BLANK END OF CLASS 1 DATA
C
```

```
C Class 2 U.M. Data Cards (Machine-Table)
C card(1)  (Type 4 note: NCLD (col 3-4) = BLANK & NCLQ (col 5-6) = BLANK
C
C
C         Mech  TACS NP     RJ           DCOEF         EPSOM         FREQ
C <-<-<<<<---><----<><-----------><-----------><-----------><----------->
 4    111ROTOR1       2                                                60.0
C .^.^^^^.....^xxxxx..^............^............^............^............^
C
C Note: "For generator operation, a positive mechanical input is required,
C       injected at 'TORINJ' passing through 'LEDRES' to 'RTMASS'"
C
C card(2)
C     OMEGM         LMUD    I      LMSD         FLXSD         FLXRD
C -----------<----------->-<-----------><-----------><----------->
                    0.18560
C ..........^............^^............^............^............^
C card(3)
C  THETAM           LMUQ    I      LMSQ         FLXSQ         FLXRQ
C -----------<----------->-<-----------><-----------><----------->
                    0.18560
C ..........^............^^............^............^............^
C card(4)
C AMPLUM-SLIP     ANGLUM      BUSF  BUSM
C ----------><------------<-----<-----<---------------------------------
         2.5                    ADJUST
C ..........^........................^
C
C Class 3 U.M. Data Cards (Coil-Table)
C stator winding (power coils, A, B, C IN 0, D-Axis, Q-Axis sequence )
C
C      RESIS       LLEAK      BUS1  BUS2 XTACSI      CUR
C -----------<------------<-----<-----<-----<<----------->
                            MOTORA           1
      0.26773     0.0017754MOTORB           1
      0.26773     0.0017754MOTORC           1
C ..........^............^.....^.....^.....^^............^
C
C shorted equivalent rotor coils, B, C, A IN D-Axis, Q-Axis, and 0 sequence)
C      RESIS       LLEAK      BUS1  BUS2 XTACSI      CUR
C -----------<------------<-----<-----<-----<<----------->
      1.14200     0.0097000BUSR_B
      1.14200     0.0097000BUSR_C
                           BUSR_A
C ..........^............^.....^.....^.....^^............^
BLANK END OF ALL UM DATA
C
```

Figure 14 - U.M. Induction Motor Model

Running the Cases

After the data files have been built, all that remains is to run enough cases, first to find any problems that may exist, and finally to find the solution to those problems. The first case run shows that when the capacitor is switched, when there are no external (except as noted above) or internal inductors, that the voltage level in the DC link exceeded the limit of 810VDC given by the vendor, meaning that the drive would trip. It can be seen in Figure 15 that the value rose to 897VDC. The customer's preferred solution was to install the internal inductor, and, in the process, to gain as much margin of safety as possible without degrading the performance of the ASD. A simple rule of thumb in the industry is that a 3% inductor will cure the majority of problems of this nature. This being the case, that was the first choice for a value to correct the problem. It's results can be seen in Figure 16. This did bring the DC link voltage within the vendor's criteria, but the customer wanted to know the effect of a 10% internal inductor. Those results are shown in Figure 17. There is more improvement, as would be expected, without signs of degradation. This was the final value chosen by the customer, since it will keep the DC link voltage well within tolerance. It will also provide some filtering of drive harmonics, and, with the safety margin, the ASDs will still operate without tripping, even if capacitor banks are added or increased in size. Next, a series of cases was run using external inductors instead of the previously used internal inductor. The results are shown in Figure 18 and their comparison appears in Table 1.

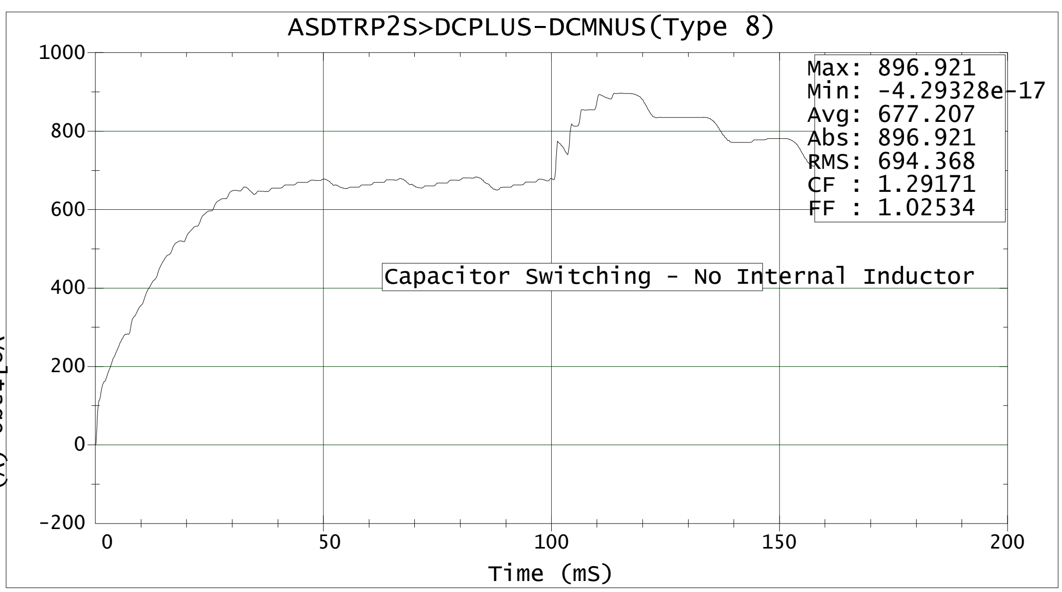

Figure 15 - Capacitor Switching - No Internal Inductor

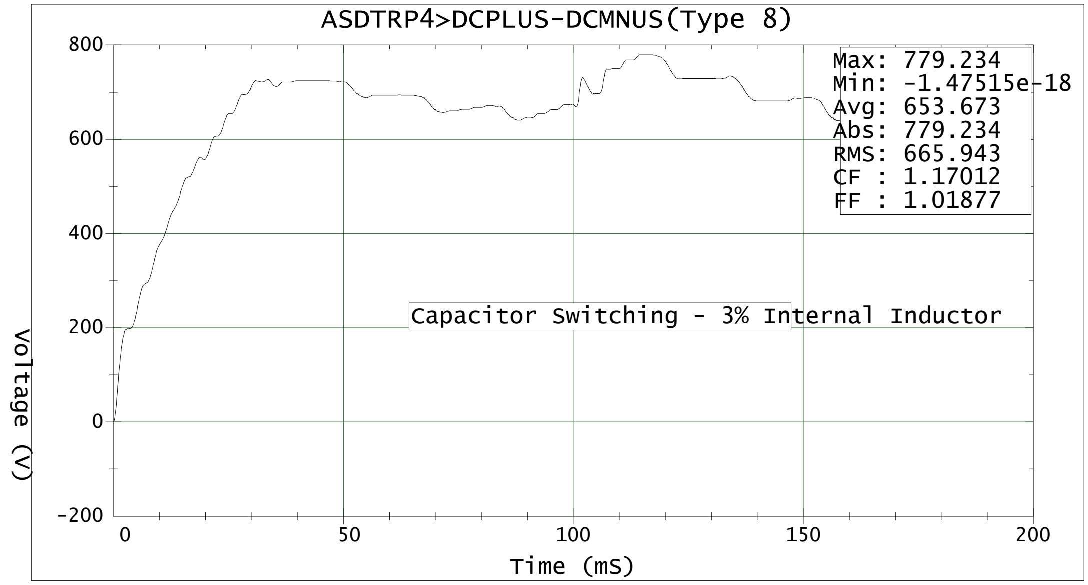

Figure 16 - Capacitor Switching - 3% Internal Inductor

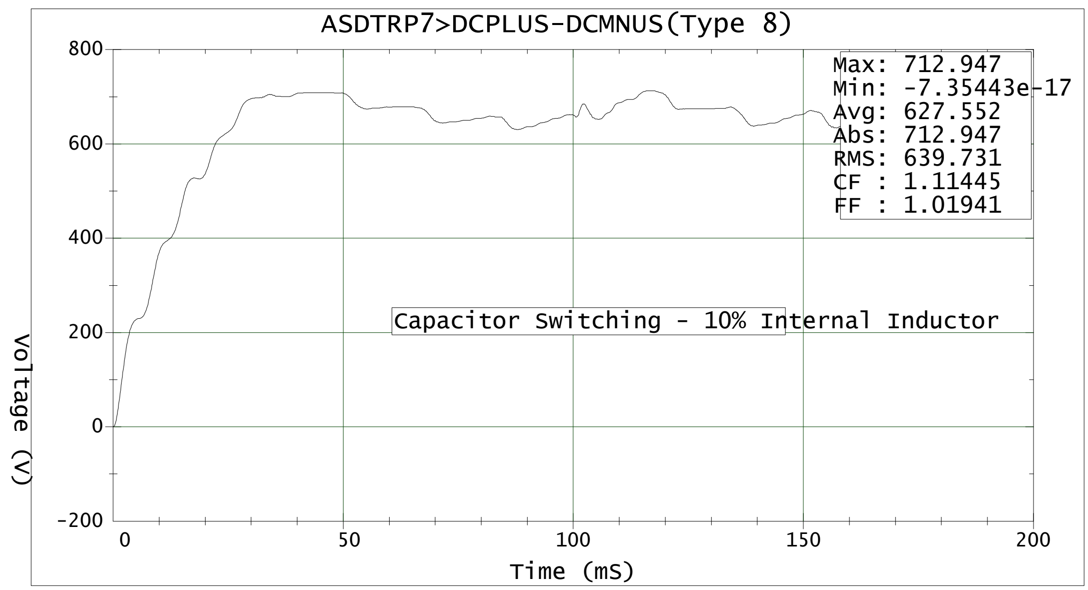

Figure 17 - Capacitor Switching - 10% Internal Inductor

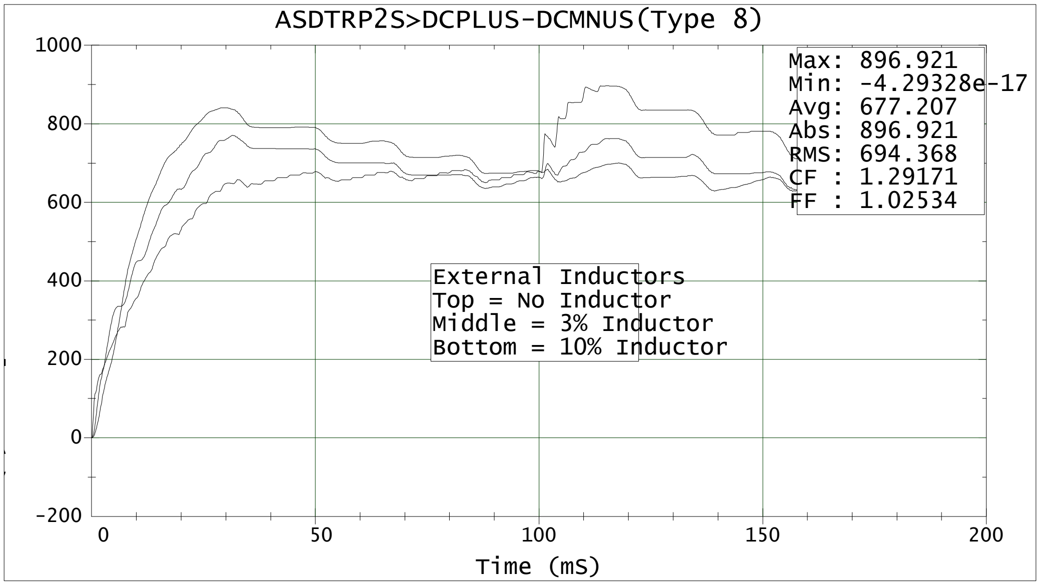

Figure 18 - Capacitor Switching - External Inductors

Table 1 - Comparison of Internal Vs External Inductors

Inductor Location	Rating	dc Link Voltage
None	0.20%	897
Internal	3.00%	779
Internal	10.00%	713
External	3.00%	771
External	10.00%	700

As noted in Table 1, using external inductors causes a slight reduction in DC link voltage versus the same value internal inductor. Therefore, placement of the inductor does affect the DC link voltage. The wave form for the 10% external inductors is beginning to show signs of degradation in the DC link and its use may not be desired.

The next exercise was to run a similar series of cases for each of the two new models, the simplified one and the U.M. induction machine. As can be seen in Figures 19 through 21, the simplified model always produced lower voltages on the DC link while the U.M. model produced results very close to the original model, although usually slightly higher.

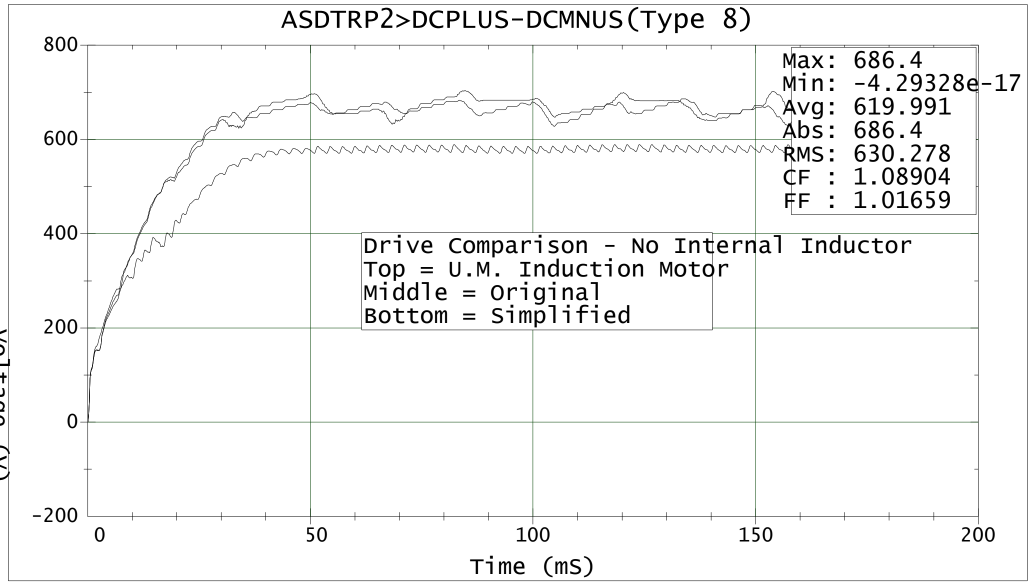

Figure 19 - Drive Comparison - No Internal Inductor

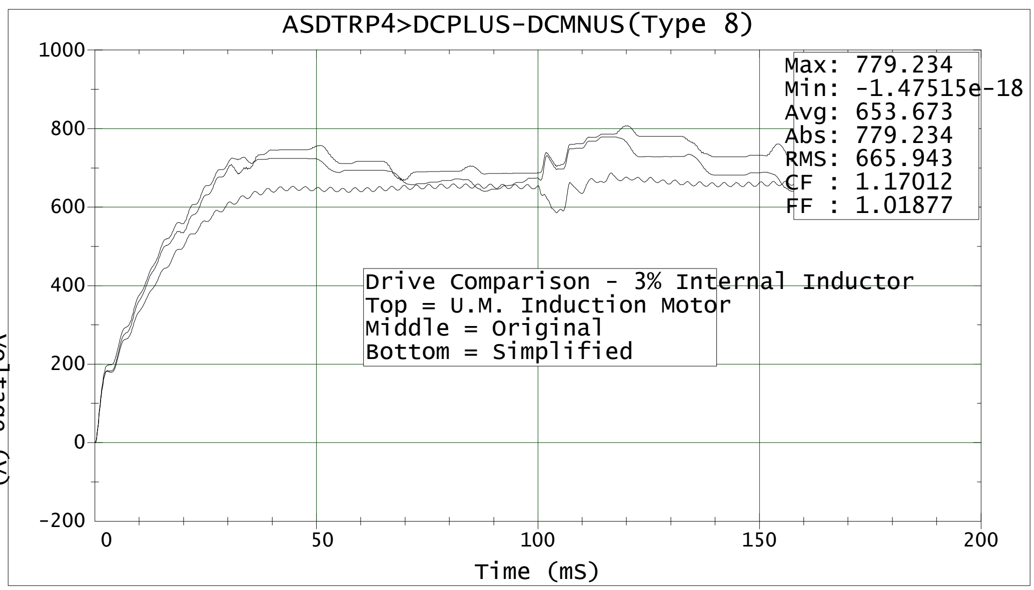

Figure 20 - Drive Comparison - 3% Internal Inductor

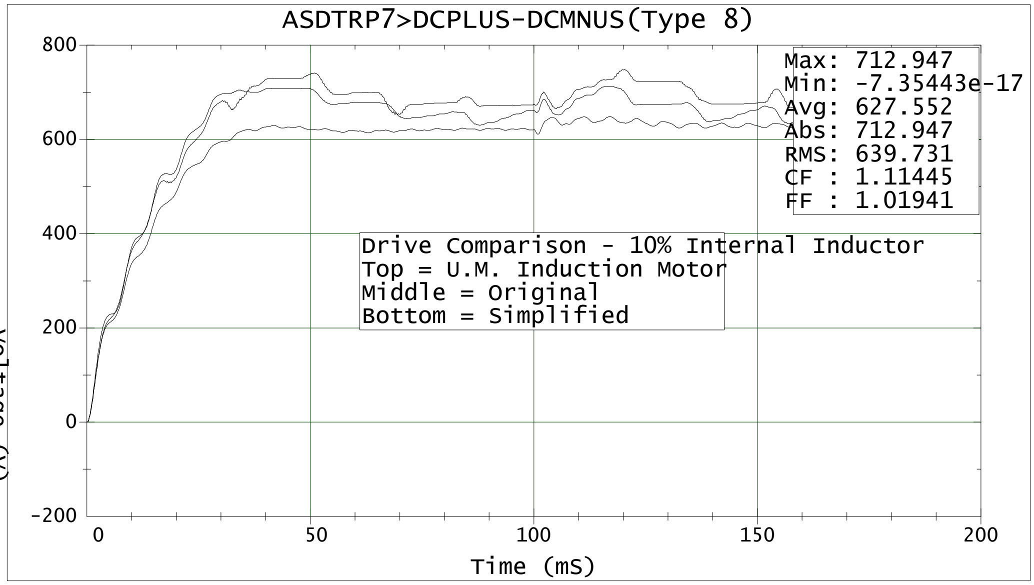

Figure 21 - Drive Comparison - 10% Internal Inductor

As a last effort, it was decided to model the ASDs with no inductor and utilize zero-crossing switching on the 115kV capacitor bank. To do this, the capacitor switch data was modified as shown in Figure 22.

```
/SWITCH
C
C BUS-->BUS--><---TCLOSE<----TOPEN<-------IE<----FLASH<--REQUEST<-----TARGET<--O
   115TA  CAPA104.174E-3      9999
   115TB  CAPB109.724E-3      9999
   115TC  CAPC115.284E-3      9999
C .....^.....^.........^.........^.........^.........^.........^...........^...^
C
```

Figure 22 - Zero-crossing Switching Times

The TCLOSE values were changed from their previous value of 100.000E-3 to a value that closely approximates the zero-crossing times for each phase. The results, as shown in Figure 23 below, are compared with the original case with no inductor and no capacitor switching. It can be seen that they track very closely, which says that this is a viable solution to the problem. It has it drawbacks, however, such as cost and the fact that if the customer installs no inductors, relying on the zero-crossing switch, that any future capacitor additions must also include a similar switch or the customer will experience problems or face an expense himself if he then has to add inductors.

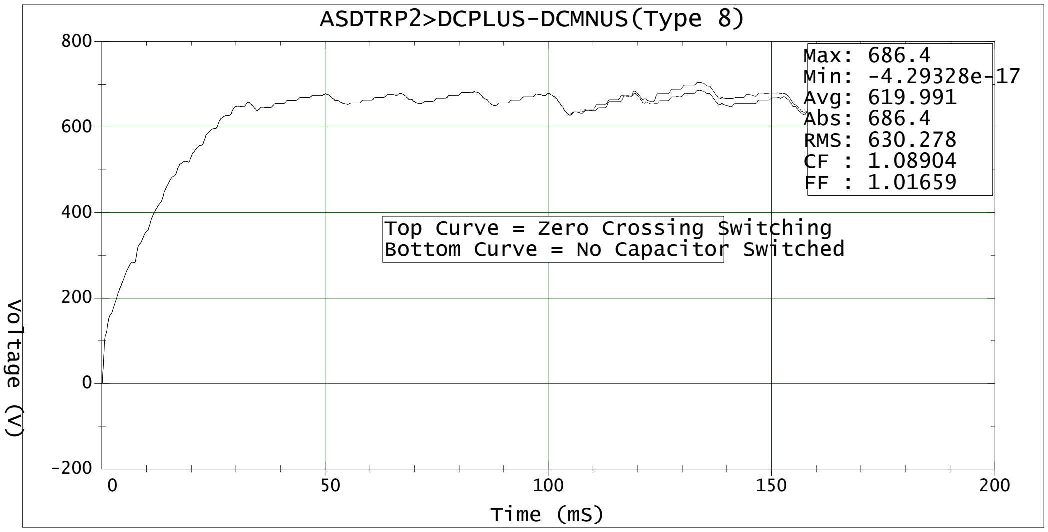

Figure 23 - Zero-Crossing Switching vs. No Switching

Conclusions

The advantage of having access to various equipment models should now be obvious. A data file that would have taken most of us untold hours just to begin was easily pieced together and utilized. The results obtained will allow us to respond to our customer in a timely manner. Along the way, we have seen that the problem could have been solved by several means. It indicates that the simplified model produced somewhat conservative results as compared to the other models. The use of the U.M. induction motor model proved to require more input and was not implemented as straight-forward as the original model, yet the results compared favorably. The use of external vs internal inductors is always an issue with customers and should be investigated, as should the use of new technology like zero-crossing switches.

As stated in the beginning, however, the main purpose of this paper was to show how an existing equipment model was utilized by an end-user. It is hoped that there are those that now have a better feel for using existing models and also that it has given model developers an insight into the "mind" of someone using their model so they can build models with the end-user in mind. It should be noted that the availability of existing equipment models made this study possible, and I doubt that this was an isolated case. Most end-users face the same limitations I do and they rely heavily on others for the needed models to perform their daily studies. I must also say that a debt of gratitude must go out to those who spend countless hours developing these models, for without them most of us would go lacking in our efforts to solve many day-to-day problems.

References

[1] EPRI/DCG EMTP User's Group, EMTP-PC Case Study Workbook, Volume 1, Draft #1, Electrotek Concepts, Inc.,1992

[2] Capacitor Energizing Transients

[3] M.F. McGranaghan, R.M. Zavadil, G. Hensley, T. Singh, M. Samotyj, "Impact of Utility Switched Capacitors on Customer Systems - Magnification at Low Voltage Capacitors"

[4] M.F. McGranaghan, R.M. Zavadil, G. Hensley, T. Singh, M. Samotyj, "Impact of Utility Switched Capacitors on Customer Systems - Part II - Adjustable-Speed Drive Concerns"

[5] Thomas E. Grebe, Le Tang, "Analysis of Harmonic and Transient Concerns for PWM Adjustable-Speed Drives Using the Electromagnetic Transients Program"

[6] Electromagnetic Transients Program (EMTP) Revised Rule Book Version 2.0, EPRI EL-6421-L

[7] Ned Mohan et al., Power Electronics: Converters, Applications, and Design. John Wiley and Sons, Inc. 1989

[8] EPRI/DCG EMTP User's Group, EMTP Case Study Workbook, Modeling and Analysis of Adjustable-Speed Drives, Electrotek Concepts, Inc., 1993

Reuben F. Burch IV
Alabama Power Company
Birmingham, Al.

EMTP Lightning Simulation

EMTP Simulation of Lighting and Arrester Operation

Introduction

Overhead transmission and distribution lines for all system voltages are exposed to lightning. Traditionally, lightning research has been directed toward formulating design and protective practices for transmission lines. However, lightning also represents a major cause of outages and equipment damage on power distribution systems.

EMTP is the only practical tool for lightning overvoltage analysis or lightning surge insulation coordination. The broad range of power system elements that can be simulated with EMTP make it ideally suitable for lightning studies. In this paper, the response of a distribution line to lightning is modeled in the following three ways:

1. With no lightning arresters,
2. With a lightning arrester on the top phase,
3. With lightning arresters on all phases.

A detail modeling guideline of all the relevant circuit elements is presented along with a parametric evaluation of the sensitivity of lightning overvoltage to parameters such as tower footing resistance, rise time, lead length, etc.

Overview

A lightning stroke is assumed to approach the earth in the vicinity of a distribution line. When the stroke tip contacts the distribution line, negative charge flows from the stroke current onto the line. This is akin to injecting a negative stroke current at the stricken point. The injection of a stroke current into a distribution circuit causes extremely high conductor-to-conductor voltages and conductor-to-ground voltages. These voltages may exceed the insulation strength between conductors and cause insulation breakdown.

Lightning overvoltages in a distribution system depend on many parameters, and a comprehensive and relatively complicated model is necessary to perform reliable calculations. All power system circuit elements must be represented in the correct way to determine the risk of failure for a given system. A realistic evaluation of the problem is primarily affected by the limited precision of the information about the lightning stroke itself. However, the recent completion of EPRI Project RP 2542-1, "Characteristics of Lightning Surge on Distribution Lines [1]," sheds some light on surge arrester discharge voltages and currents caused by lightning.

Data Required for EMTP Model

The following data must be assembled to simulate lightning with EMTP:

- Design parameters of the distribution circuit, i.e. pole configuration, physical conductor data, etc.
- Tower surge impedance, or in case of a wooden pole, ground lead surge impedance.
- Tower footing resistance.
- Grounding interval.
- Arrester rating, along with its discharge characteristics.
- Arrester lead length.
- Characteristics of the lightning stroke, i.e. peak current, front time, and tail time.

The procedure for assembling the data is described in this section.

Lightning Stroke

The stroke current amplitude within a lightning flash is described in terms of probabilities [2]. The waveshape of the stroke current is defined in terms of a peak value, a front time, and a tail time, as shown in Figure 1. The wave front and wave tail can be simulated with straight lines in EMTP by using source type 13 [3]. However, if the discontinuity in slope at the peak and zero values leads to spurious oscillations, then double exponential source type 15 can be used as an alternate. An iterative procedure determines the value of the exponents for source type 15. Since peak current, front time, and tail time are statistical in nature, a Monte Carlo simulation is required to properly study the problem.

Figure 1 - Input Lightning Current Surge

Description of the Model Distribution System

For illustration purposes, a 12.47 kV distribution line with four spans, shown in Figure 2, is modeled during a direct strike to a conductor at pole number 3. Lightning performance of the distribution line is studied, using each of the following protection strategies:

1. No lightning protection.
2. Line equipped with an MOV arrester on the top phase of pole no. 3.
3. Line equipped with MOV arresters on all phases at pole no.3.

For each of these strategies, a lightning stroke at the top phase (i.e. conductor *2), and a lightning stroke at one of the bottom phases (i.e. conductors *1 or *3), are simulated.

The characteristics of the system and event are

a) Pole configuration and line data as shown in Figure 3.
b) Travel time between spans = 0.25 µsecs.
c) No propagation losses.
d) Ground lead surge impedance = 390 ohms.
e) Pole footing resistances of 20, 20, 1.8, 20, and 20 ohms for poles 1-5, respectively.
f) Lightning stroke current wave shape is standard 8 x 20 µsec ramp (i.e. 8 µsec front time, 20 µsec tail time),
g) Peak current magnitude = 10 kA.
h) 10 kV MOV characteristics, based upon standard 8 x 20 data, as shown in Table 1.

*Figure 2 - Lightning Stroke at Top Phase (i.e. Conductor *2) of Pole No. 3, with an MOV Arrester*

Figure 3 - 12.47 kV Line Data and Pole Configuration

Table 1 - MOV Characteristics at 10 kV

Line Model

Figure 3 shows the line configuration along with the physical 12.47 kV line data. The EMTP Line Constants Program is used to generate the required line data according to Lee's line model [3], using the input data file shown in Appendix A. The ground wire is retained in the model. Line parameters are calculated at 500 kHz to be more representative of lightning surges, and the following high frequency lossless approximations, which are relevant to lightning studies, are made:

- Zero penetration depth in the conductor. This is realized by setting GMR/r = 1 for the conductors. In the Line Constants Program, placing a 3 in column 18 of the conductor data card, and setting REACT = 1.0, ensures zero penetration.
- Zero earth return depth. This assumption is implemented by placing a 0 in column 28 of the frequency card, thereby bypassing Carson's equations.
- Zero conductor and earth return losses. Bypassing Carson's equations ensures zero earth return loss and makes the input value of earth resistivity irrelevant. Zero conductor loss is implemented by placing a 2 in column 70 of the frequency card.

A portion of the Line Constants Program output is shown in Appendix A. The output needed for lightning simulation are

- Traveling wave parameters
- Modal transformation matrix.

- Surge impedance matrix in phase domain.

Arrester Model

There are two fundamental ways to represent lightning arresters with EMTP. These are:

- Use of point-by-point nonlinearities (i.e. piecewise-linear segments).
- Use of built-in ZnO model.

Point-by-point nonlinearities are specified in EMTP input files as type 92 (true nonlinearity), or type 99 (pseudo-nonlinearity). Point-by-point arrester modeling requires the fixed series resistance, flashover voltage, and set of v-i points describing the arrester characteristics. For the example given in this section, the 10 kV MOV is modeled point-by-point using manufacturers 8x20 μsec data from [1].

Another way of representing a lightning arrester is with the built-in model of a ZnO surge arrester (type 92, code 5555) model. ZnO arresters are highly nonlinear resistors whose I-V characteristics are governed by

$$I = p\left(\frac{V}{V_{ref}}\right)^{q} \qquad (1)$$

where I is the arrester current, V is the arrester voltage, and p, V_{ref}, and q are arrester constants.

Data for distribution arrester (3–24 kV, 10 kA rating) lightning discharge currents, measured on the South Africa 11 kV test line project [4], show that several sizes and manufacturer types of arresters can be described by an equation given in [5], which is

$$\frac{V}{V_{ref}} = 2.5 \bullet I^{q} \qquad (2)$$

where

q: exponent of nonlinearity (ranging from about 0.1 to 0.25).

V: residual voltage across the arrester in kV.

I: discharge current through the arrester in kA.

Vrms: arrester power frequency voltage rating in kV.

By comparing (2) to (1), and by substituting the above values, the coefficients in (1) become V_{ref} = Vrms, p = 0.4, q = 4 to 10.

System Modeling Rules

Figure 4 shows the complete EMTP model for simulating a lightning strike at a bottom phase (conductor *1) of pole 3 with an arrester on the top phase. The corresponding EMTP input data file is presented in Appendix B. The modeling rules are:

- Since the distribution line and poles are symmetric about the struck pole, the lines can be folded at pole 3 so that they are in parallel, with a combined one-half of their individual characteristic surge impedance. This implies that the lightning current divides equally in both directions.
- The line beyond pole 5 is represented by its surge impedance termination matrix obtained from the Line Constants Program output.
- Ground leads are represented by a surge impedance of 390 ohms and a travel time corresponding to the 28 ft. lead length at the speed of light.
- The ground lead of pole 3 has its normal surge impedance and footing resistance, while the phase and ground conductors, as well as the other pole ground leads and footing resistances, are halved in value.
- The ground lead surge impedance is connected in series with an earthing impedance system. The three choices for modeling earthing impedance are:
    1. constant resistance.
    2. time varying resistance.
    3. current dependent resistance.

In our present model, the tower footing impedance is represented by a constant resistance whose value is changed in discrete steps to determine its effect on lightning overvoltages for different type of protection schemes. Reference [6] deals in depth on the proper selection of pole footing resistance. The current- and time-dependent models account for the effect of soil breakdown. These models are based on references [6] and [7].

The time step must be chosen so that it is less than the travel time of the shortest conductor section, which for this example is the ground lead. The overhead span travel time is 0.25 msec for all three modes. The ground lead travel time corresponds to 28 ft. lead length at the speed of light, or 0.0284 msec. Ideally, there should be an integer number of time steps for each of the travel times in the problem, or else a very large number of time steps. For this example, a time step of 0.012 msec is chosen, which provides twenty-one time steps for the overhead span modes.

*Figure 4 - EMTP Model for a Lightning Strike to Bottom Phase (i.e. Conductor *1) at Pole 3*

Simulation and Discussion of the Results

Now that the data are assembled, EMTP is used to simulate lightning strikes on different phases and for different arrester configurations. First, consider a direct 10 kA, 8x20 µsec strike at the top phase conductor at pole 3. Figures 5 and 6 show the voltage waveshapes at pole 3, without and with an arrester installed on the top phase, respectively. The top phase arrester reduces the overvoltages on all the phase conductors by more than by 95%.

Figure 5 - Voltage Waveshapes at Pole 3 with no Arresters (Strike at Top Phase)

Figure 6 - Voltage Waveshapes at Pole 3 with Arrester on Top Phase (Strike at Top Phase)

Although rare in transmission circuits, the most common lightning event in distribution circuits is an induced strike, where lightning hits the ground nearby, and the return stoke hits the bottom phase conductor (see page 483 in [8]). This is simulated as a positive-polarity direct strike on the bottom phase conductor. Figures 7 and 8 show the resulting overvoltage magnitudes. These figures indicate that the arrester on the top phase is unable to reduce the overvoltage due to an induced strike.

Figure 7 - Voltage Waveshapes at Pole 3 with Arrester on Top Phase (Strike at Bottom Phase)

Figure 8 - Voltage Waveshapes at Pole 3 with Arresters on All Phases (Strike at Bottom Phase)

The peak overvoltages for the simulations described in Figures 5 - 8 are summarized in Table 2.

Table 2 - Peak Lightning Overvoltages in kV

Parametric Variations

Peak lightning overvoltage magnitude depends on parameters such as tower footing resistance, spacing between grounded poles, arrester lead length, stricken location, and the characteristics of the lightning stroke. The effect of some of these parameters for a lightning stroke at pole 3 is illustrated in the following subsections. Cases with and without an arrester on the top phase are considered.

Effect of Pole Footing Resistance

The effect of pole footing resistance is observed by varying it in discrete steps over a range of 5 - 40 ohms. The results are shown in Figures 9 and 10, where it is observed that the phase conductor voltages for the no-arrester case do not depend on pole footing resistance. This is expected since the stricken phase is not connected to ground in any way. As expected, the voltage on the ground wire increases as the footing resistance increases.

Figure 9 - Effect of Footing Resistance on Conductor Overvoltages (No Arrester)

Figure 10 - Effect of Footing Resistance on Conductor Overvoltages (Arrester on TOP Phase)

However, when the stricken phase is grounded through an arrester, all conductor voltages increase with pole footing resistance increases.

Effect of Rise Time

The rise time of stroke current is varied from 1 µsec to 8 µsec in steps of 1 µsec. The simulation results are shown in Figure 11. When no arrester is present, the maximum overvoltage in the top phase is unaffected by rise time. However, when an arrester is present on the top phase, the overvoltage increases as rise time decreases. This is due to reflections from the ground footing resistance which is now connected to the stricken phase through the arrester.

Figure 11 - Effect of Rise Time on Top Phase Overvoltage

Effect of Arrester Lead Length

Additional arrester lead length decreases the level of protection. Figure 12 shows the effect of lead length on the top conductor overvoltage when a steep-fronted (2x20) surge is injected into it at pole 3.

Figure 12 - Effect of Lead Length on Top Phase Overvoltage

Effect of Tail Time on Arrester Energy Dissipation

Due to their short duration, lightning phenomenon do not usually pose a problem for arrester energy dissipation capability. Manufacturers often rate their arrester energy dissipation capabilities 2.2 kJ per kV of maximum continuous operating voltage (MCOV). However, a more conservative estimate of the discharge capability of heavy-duty MOV arrester is 1.5 kJ per kV of MCOV [9].

Induced surges in distribution circuits have a long decay time, and this may result in considerably higher energy discharge levels in arresters than normally expected. This effect is studied by varying the tail time of a 10 kA stroke from 20 msec to 80 msec in steps of 10 msec. Figure 13 shows the energy dissipation for a 10 kV arrester, where it is quite evident that this energy can be higher than 1.5 kJ per kV for long tail times.

Figure 13 - Effect of Tail Time on Energy Dissipation in 10 kV MOV Arrester

References

[1] P. P. Barker, T. M. Mancao, D. J. Kvaltine, D. E. Parrish," Characteristics of Lightning Surges Measured at Metal Oxide Distribution Arresters", *IEEE Trans. on Power Delivery,* vol. 8, no. 1, January 1993.

[2] J. G. Anderson, "Lightning Performance of Transmission Lines," chapter 12 of *Transmission Line Reference Book – 345 kV and Above*, 2nd edn., EPRI, 1982.

[3] "Electromagnetic Transients Program (EMTP) Revised Rule Book," version 2.0, vol. 1, vol. 2, EPRI EL-6421-L, EPRI/DCG, June 1989.

[4] A. J. Eriksson, M. F. Stringfellow, D. V. Meal, "Lightning Induced Overvoltages on Overhead Distribution Lines," *Trans. IEEE*, vol. PAS-101 , pp. 960-968, 1982.

[5] H. J. Geldenhuys, M. F. Stringfellow, D. V. Meal, " Measured Lightning Discharge Duty of Distribution Surge Arresters", *IEE Conference Publication Number 236.*, 1984.

[6] A. C. Liew, M. Darweniza, " Dynamic Model of Impulse Characteristics of Concentrated Earths", *Proc. IEE*, vol. 121, no. 2, pp. 123-125, 1974.

[7] E. R. Whitehead, "Circuit Models for the Response of Tower and Grounding Systems in the Estimation of Backflash Lightning Performance", *Report to SC 33 Colloquium 1983*, Edinburgh.

[8] A. N. Greenwood, *Electrical Transients in Power Systems,* John Wiley & Sons, Inc., New York, 1991.

[9] E. C. Sakshaug, J. J. Burke, J. S. Kresge, "Metal Oxide Arresters on Distribution Systems - Fundamental Considerations", *IEEE Transaction on Power Delivery*, vol. 4, no. 4, October 1989.

Mack Grady
Arshad Mansoor
Department of Electrical and Computer Engineering,
University of Texas at Austin

APPENDIX A (EMTP AUXILIARY DATA FILES)

Line Constants Data File (ARSTR1.DAT)

```
BEGIN NEW DATA CASE
C    SECTION 2
C    DATA FILE = 'ARSTR1.DAT'
LINE CONSTANTS
LINE-PARAMETERS
ENGLISH
C    LINE CONSTANTS FOR THE 12.47 kV DISTRIBUTION LINE
C    LINE PARAMETERS AT 500 kHz
C    GROUND CONDUCTOR IS RETAINED AS THE 4th CONDUCTOR
    1      0.0     .000    3      1.0     .710    0.0     31.33
    2      0.0     .000    3      1.0     .710    3.667   32.58
    3      0.0     .000    3      1.0     .710    7.334   31.33
    4      0.0     .000    3      1.0     .502    3.667   28.00
BLANK CARD TERMINATING CONDUCTOR CARDS
C   FREQUENCY CARD
           1.0  500000.                  0      1        1.0
2
BLANK CARD TERMINATING FREQUENCY CARDS
BLANK CARD TERMINATING LINE CONSTANTS CASES
BLANK CARD TERMINATING THE CASE
```

```
PORTION OF LINE CONSTANTS OUTPUT
MODAL PARAMETERS AT FREQUENCY  FREQ = 5.00000000E+05 HZ

                        MODE    SURGE IMPEDANCE
                                  (OHMS/MILE)
                          1       9.22956E+02
                          2       2.78183E+02
                          3       3.21818E+02
                          4       3.30147E+02
EIGENVECTOR MATRIX  [Q]  FOR CURRENT TRANSFORMATION:  I-PHASE = [Q]*I-MODE.
FIRST THE REAL PART, ROW BY ROW:

       4.865976E-01   4.576900E-01  -2.318244E-01  -7.071067E-01
       5.233174E-01  -7.557604E-01  -3.936559E-01  -3.300542E-15
       4.865976E-01   4.576900E-01  -2.318244E-01   7.071067E-01
       5.025777E-01  -9.932626E-02   8.588072E-01   3.870403E-15

Z-SURGE IN THE PHASE DOMAIN.  RESISTANCE AND THE IMAGINARY PART OF•• [Q]  ARE
IGNORED.

       4.591782E+02
       1.681704E+02  4.615239E+02
       1.290310E+02  1.681704E+02  4.591782E+02
       1.489941E+02  1.548287E+02  1.489941E+02  4.732260E+02
```

APPENDIX B (EMTP INPUT DATA FILE)

Data File for Lightning and Arrester Operation (ARSTR2.DAT)

```
BEGIN NEW DATA CASE
C  SECTION 2
C  DATA FILE = 'ARSTR2.DAT'
C  LIGHTNING STRIKE AT COND. 1 OF POLE 3.
C  ARRESTER INSTALLED AT CONDUCTOR 2.
C  LINE TERMINATED WITH SURGE IMP. TERMINATION MATRIX
C  STANDARD 10 kA, 8 x 20 CURRENT SURGE
C  START OF TIME DATA
 1.20E-8 20.0E-6  60.    0
   40000     100       1       1       1                       1
C TERMINATING SURGE IMPEDANCE AT THE END OF THE LINE
 1P5-C1                  229.50
 2P5-C2                  84.000           230.75
 3P5-C3                  64.500           84.000           229.50
 4P5-GR                  74.45            77.4             74.45
                              236.5
C TOWER FOOTING RESISTANCES
  P3GRND                 01.80
  P4GRND                 10.00
  P5GRND                 10.00
C GROUNDING LEAD MODELED AS CONSTANT DISTRIBUTED PARAMETER
-1P3-GR P3GRND           0.0   396.0  9.8E8 28.00 1
-1P4-GR P4GRND           0.0   198.0  9.8E8 28.00 1
-1P5-GR P5GRND           0.0   198.0  9.8E8 28.00 1
C ARRESTER CONNECTION TO THE TOP PHASE
  P3-C2 ARRST1                 9.0E-4
92ARRST1P3-GR                         4444                                 4
  0.0                     18.0                     0.0
          1E-3                  18.060
         10E-3                  18.940
        100E-3                  20.570
       1000E-3                  23.380
       1500E-3                  24.450
      10000E-3                  29.600
      20000E-3                  33.150
      50000E-3                  38.550
        9999
C UNTRANSPOSED LINE MODEL USING THE KC LEE LINE MODEL
$VINTAGE, 1
-1P3-C1 P4-C1             0.0         461.45     186280.     -.0465      1  4
-2P3-C2 P4-C2             0.0         139.10     186280.     -.0465      1  4
-3P3-C3 P4-C3             0.0         160.90     186280.     -.0465      1  4
-4P3-GR P4-GR             0.0         165.00     186280.     -.0465      1  4
$VINTAGE, 0
  0.48659760   .45769007  -.23182443  -.70710678
  0.0           0.0        0.0         0.0
  0.52331740  -.75576047  -.39365594   0.0
```

```
  0.0           0.0        0.0
  0.48659760  0.45769007  -.23182443   .70710678
  0.0         0.0          0.0
  .502577791  -.09932626  .858807228   0.0
  0.0         0.0           0.0        0.0
$VINTAGE, 1
-1P4-C1 P5-C1 P3-C1 P4-C1
-2P4-C2 P5-C2 P3-C2 P4-C2
-3P4-C3 P5-C3 P3-C3 P4-C3
-4P4-GR P5-GR P3-GR P4-GR
BLANK CARD ENDING BRANCHES
C SWITCH CARDS
C T1-GW T1-PH  1.0                                                          2
BLANK CARD TERMINATING SWITCHES
C SOURCE CARDS
13P3-C1 -1   10.                   8.E-6   5.0      20.E-6  0.0
BLANK CARD TERMINATING SOURCE CARDS
C NODE OUTPUT VOLTAGE REQUEST
  P3-C1 P3-C2 P3-GR
BLANK CARD TERMINATING NODE VOLTAGE OUTPUT
BLANK CARD TERMINATING PLOT REQUEST
BLANK CARD TERMINATING THE CASE
BEGIN NEW DATA CASE
```

Capacitor Bank Analysis

Innovations for Protection and Control of High Voltage Capacitor Banks on the Virginia Power System

Introduction

Two new capacitor bank designs were added to the Virginia Power transmission network last year. These capacitor bank applications, one 500kV fused design and one 230kV fuseless, are presented as examples of developments in the design and protection of grounded shunt capacitor bands. The 500kV design is the first on the Virginia Power 500kV network. The fuseless capacitor bank is the first 230kV bank of this type in the country.

The Morrisville 500kV capacitor bank was added to provide MVAr capacity during bulk power transfers across the northern part of the 500kV network. The addition of the capacitor bank prevents the requirement to start an 882 MW oil fired generating unit under non-economic dispatch just to provide voltage support for the bulk power transfer. The reduced fuel costs could repay the cost of the capacitor bank in only a few years.

The Yorktown 230kV fuseless capacitor bank was added to provide MVAr capacity to a peninsula area with limited transmission access near the Atlantic Ocean. Because of the limited transmission access heavy loads required the running of another 882 MW oil fired generating plant for voltage reasons before it was required by economic dispatch. The proximity to the salt water contamination, past problems with fuse failures, and limited space in the substation made this application an ideal site for a fuseless bank.

This paper describes the transient design, relay protection, zero voltage closing control, and operating problems associated with the capacitor bank design and operation.

Morrisville 500kV Capacitor Bank

Overview

The Morrisville capacitor bank was sized at 367.5 MVAr @ 552.9kV. There were 1050 - 350 kVAr capacitor units each rated at 22.8kV. These capacitors were arranged in 14 series groups per phase, with 25 cans per group. Each capacitor unit was protected with a current limiting fuse in series with a 25 ampere K-link. The current limiting fuses were required due to the amount of parallel energy discharged during a unit failure.

The capacitor switch was a SF_6 live tank breaker, rated at 550kV, with a 3000 ampere continuous rating. The breaker was equipped with 200 ohm closing resistors per phase and a microprocessor based relay for synchronous closing operation. Although the switch was capable of withstanding the outrush current during a nearby fault, reactors were installed. The outrush reactors were required to protect the existing 500kV air blast breakers in the station. Metal oxide arresters (MOVs), sized at 396kV were installed to limit overvoltages caused by a possible restrike of the capacitor breaker.

EMTP Simulations and Results

There are a several important transient related concerns when transmission voltage level capacitor banks are applied. The transmission system concerns include insulation withstand level, switchgear capabilities, energy duties of protective devices, and system harmonic considerations. Often, these considerations need to be extended to include the distribution systems and sensitive customers. Considerations for the Morrisville 500kV application included:

- Overvoltages associated with normal capacitor energizing
- Open line/cable end transient voltages
- Phase-to-phase transients at transformer terminations
- Voltage magnification at lower voltage capacitor banks
- Arrester duty considerations
- Analysis of current limiting reactor requirements
- System frequency response and harmonic injection
- Impacts on sensitive customer loads
- Analysis of ferroresonance possibilities

Transients associated with normal energizing of the Morrisville 500kV capacitor bank were evaluated using an extensive EMTP model. The model consisted of the entire Virginia Power 500kV system, part of the 230kV system, and several distribution substations and feeders. Figure 1 illustrates the worst case phase transient voltage for normal energization of the 367.5 MVAr bank.

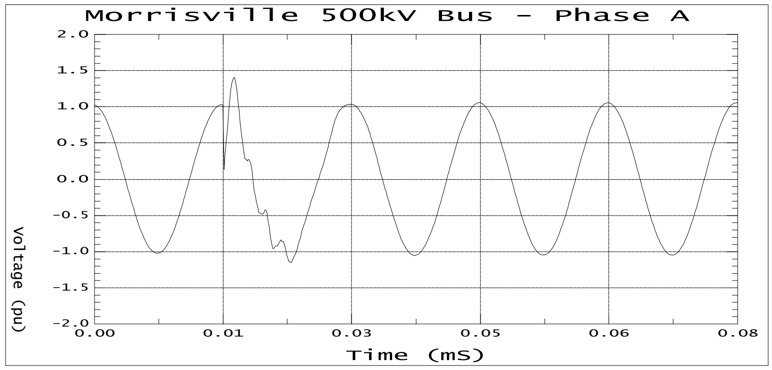

Figure 1 - Transient Voltage During Normal Energizing

Simulation results indicated that several factors would affect the severity of the transient overvoltage during normal energizing. These factors include:

Source strength: The transient became more severe as the source strength was reduced. Typically, when the source short circuit capacity is relatively low, compared to the size of a capacitor bank, the disturbance caused by the capacitor energizing is the most dramatic.

Transmission lines: Transmission lines and their associated capacitance reduced the capacitor bank energizing transient. In general, transmission line capacitance effectively makes the system "stronger" for the energizing operation. The exchange of energy between the line capacitance and the capacitor bank occurs at a wide range of frequencies. Combined, these frequencies tend to damp the overall transient.

Other transmission system capacitor banks: Shunt capacitor banks, near the switched capacitor bank, reduced the system surge impedance and made the equivalent short circuit capacity of the source stronger. This reduced the energizing transient somewhat. Typically, capacitor banks spread over the system absorb energy associated with the initial transient and help to reduce overall transient overvoltage on the system.

Switching device: Control of the energizing transient was evaluated using preinsertion devices (resistors or reactors) and asynchronous closing.
The optimum resistance value, for controlling capacitor energization transients, depends primarily on the capacitor size and the source strength. It should be approximately equal to the surge impedance formed by the bank and source:

$$R_{optimum} = \sqrt{\frac{L_{source}}{C_{bank}}} = \sqrt{\frac{41.1\text{mH}}{3.2\mu\text{F}}} \approx 110\Omega \quad (1)$$

Due to breaker limitations, a preinsertion resistance value of 200Ω was chosen. The addition of the preinsertion resistor reduced the transient voltage from 1.41pu to 1.06pu (note 1pu = peal phase-to-ground voltage).

Another option evaluated was synchronous closing control. Synchronous closing is independent contact closing of each phase near a voltage zero. To accomplish synchronous closing at or near a voltage zero (avoiding high prestrike voltages) it is necessary to apply a switching device that maintains a dielectric strength sufficient to withstand system voltages until its contacts touch. Although this level of precision is difficult to achieve, closing consistency between ± 0.5 msec should be possible. Simulation results showed an overvoltage range of 1.07 - 1.34pu for a synchronous closing error of 0 - 2 msec.

The scheme selected for optimum control of energizing transients consisted of a hybrid combination of synchronous closing and preinsertion resistor. Optimum performance, evaluated by simulation, was achieved by energizing the preinsertion contact at a system voltage zero and delaying the

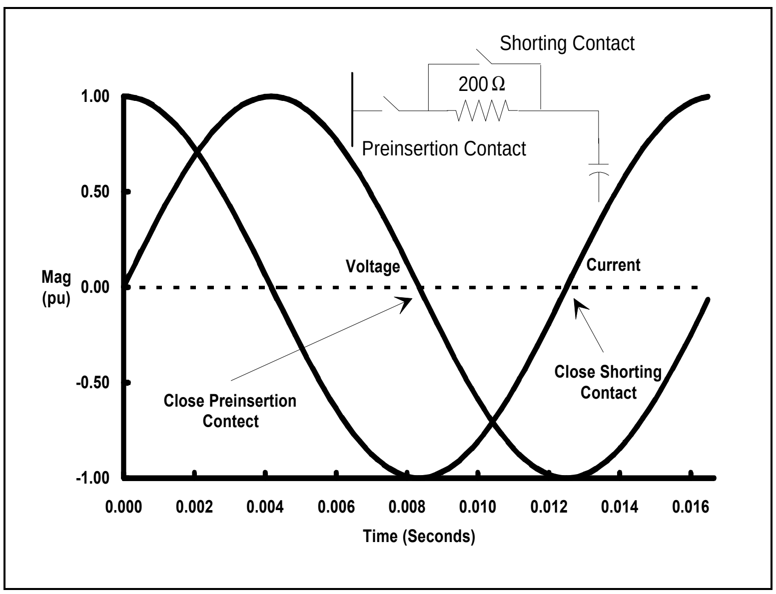

Figure 2 - Capacitor Breaker Closing Sequence

shorting contact ¼ cycle (4.1667msec). This condition energizes the capacitor at a voltage zero and shorts the resistor at a current zero (voltage zero across resistor). This sequence is illustrated in Figure 2.

Morrisville Relay Protection Scheme

A voltage differential monitoring scheme was used as the primary protection for the capacitor bank. The voltage differential scheme consists of two meter accuracy capacitor coupled voltage transformers (CCVTs) per phase connected to a microprocessor based voltage differential relay. The microprocessor relay monitors the secondary voltage from the 500kV bus CCVT and the 230kV tapped CCVT on a per phase basis. A differential voltage will occur when a capacitor unit fails causing the 230kV tapped CCVT voltage to change when compared to the 500kV CCVT voltage. Three separate voltage magnitude differential units per phase are used to detect capacitor can failures. In addition to the differential units, the relay also has three single phase overvoltage units, three single phase undervoltage units, and a maximum phase overvoltage unit. Mask programmable output logic is used to control the output contacts for tripping and event reporting. The relay also generates an eleven cycle event report when the tripping units pickup, and has RS-232 ports available for communications.

The voltage differential scheme was preferred for the Morrisville bank because it is immune to inherent system unbalances. It was estimated that a 1% system unbalance exists due to the untransposed 500kV transmission network. The scheme also filters out harmonics when it differentially compares the CCVT voltages. This makes the scheme less sensitive to solar magnetic disturbances, which were a problem recently.

Normally, transmission level capacitor banks on the Virginia Power system are designed so that two capacitor units per series group can fail before exceeding the nameplate capacitor unit voltage rating by 10%. For maximum availability, the Morrisville capacitor bank was designed to allow four units per series group to fail before 110% overvoltage was reached. At 500kV, the individual capacitor unit overvoltage is 90% of the nameplate rating of 22.8kV. A single capacitor unit failure causes the group overvoltage to rise 4%, while producing only a 0.3% voltage differential change. The differential alarm unit was set to detect a single can failure and activate a station annunciator alarm after a three minute delay. Tripping of the capacitor bank would require that the series group overvoltage exceed 110%. Four capacitors per series group would have to fail before 110% overvoltage was reached. A 1.3% voltage differential change results from the failure of the fourth capacitor unit. The differential trip unit was set to pickup when the fourth capacitor unit failed.

To detect high magnitude voltage unbalances, the high set differential unit was set to pickup for one-half of the differential voltage equivalent to a short of one of the series groups. The differential trip unit and high set unit are "masked" to trip the capacitor bank lockout relay and remove the bank from service.

The phase overvoltage and phase undervoltage units monitored the steady state voltage on the 500kV system that would be in excess of the capacitor unit voltage rating of the bank. Instantaneous tripping would occur if the steady state voltage on the 500kV system exceeded 120% of the capacitor unit voltage rating of the bank. The definite time overvoltage unit would provide timed delay tripping for steady state overvoltages in excess of 110% of the capacitor unit voltage rating of the bank.

The phase undervoltage units were set to detect a steady state undervoltage condition on the 500kV system, The undervoltage unit settings were time coordinated with the existing 500kV line protection to allow the line protection to initially clear any close-in faults. Should the primary line protection be slow to clear the fault, the undervoltage unit would time out and directly trip the breaker without operating the lockout relay. Directly tripping the capacitor bank breaker without operating the lockout allows the capacitor bank to be remotely closed back in if it is needed.

The capacitor bank has been monitored closely since its release in the Summer of 1992. Field data and operating experience has indicated that relay accuracy CCVTs could be used instead of meter accuracy CCVTs for future applications.

Field Testing of the Zero Voltage Closing Control

One of the major innovations of the Morrisville 500kV capacitor bank control is the combination of a preinsertion resistor with a zero voltage closing control to minimize the closing transients. The 500kV circuit breaker used to switch the capacitor bank has independent pole closing controls which are initiated by a zero voltage closing relay. Due to the critical application of the capacitor bank, it was decided to provide a backup to the zero voltage closing by using a preinsertion resistor.

After extensive transient simulations it was decided to recommend that the zero voltage closing control be used to close the preinsertion resistor contact then short the main contacts one-fourth cycle later. This sequence would minimize the preinsertion resistor switching transient and close the shorting contacts on a zero current crossing one-fourth cycle later. This provides excellent transient protection and if the zero voltage closing off of it automatically inserts the preinsertion resistor to minimize the closing transient.

The basic principal of the zero voltage closing control, illustrated in Figure 3, is to measure the zero voltage point, predict the total closing time of the contacts from the close initiation, calculate the time to initiate closing, and initiate close for a targeted zero voltage. In order for this scheme to work the independent pole breaker closing time must be relatively insensitive to ambient temperature, operating voltage, and aging. Since breaker mechanisms are affected by these variables to some extent, the zero voltage closing control was made to adapt to the slow change of these closing times. The tolerance target for this control device was to keep the closing time within 1msec of the actual zero voltage closing point.

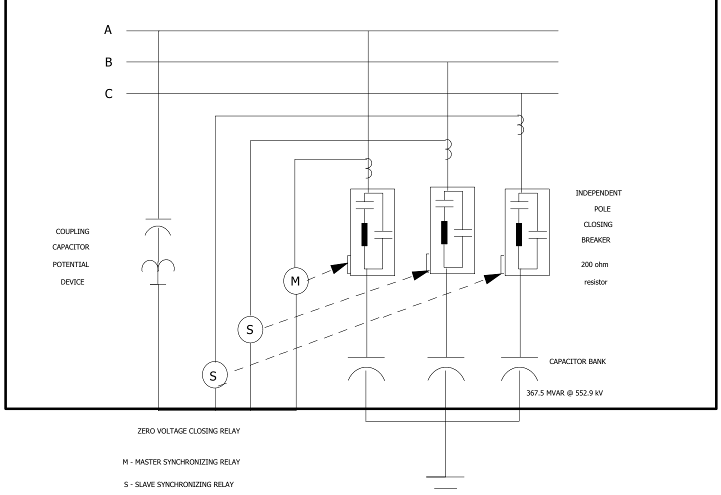

Figure 3 - Zero Voltage Closing Control

The zero voltage closing relay uses the voltage measurement from phase A to determine the zero voltage crossover. It projects the time of contact closing using the contact closing time, auxiliary relay time, and the pre-arcing time. The closing time is used to initiate close of the master phase so it will close at a voltage zero. The relay uses the current through the breaker to determine when the contacts actually close and corrects the prediction time for the next closure. This allows the relay to track any slow changes in the breaker closing times. The main contacts shorting the resistor are closed in 8-10 msec after the resistor contact closes. This is not as good as the optimum one-fourth cycle but as can be seen from Figure 3, this does not create any transient problems for the closing. The two slave relays use the initiation of the A phase closure to initiate the remaining contact closes at a zero voltage intervals one-sixth of a cycle apart.

Figure 4 illustrates the current and voltage waveforms during a closing operation. The current initiation occurs within the 1msec tolerance of the relay but without much margin for error. The closing of the main contacts can be seen around 10 msec after the current initiation.

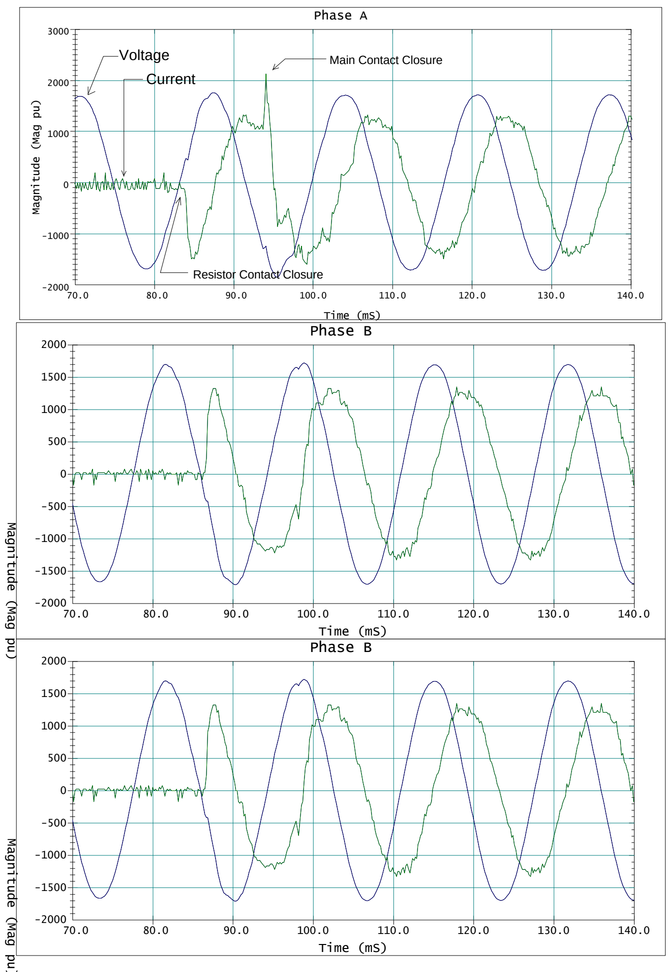

Figure 4 - Field Recording Illustrating Zero Voltage Closing Control

There was one main change made to the scheme as a result of the field testing. A remote alarm reset was added to allow the System Operator to remotely reset the alarm for an out of tolerance close. It was found that the alarms would routinely occur for large transitions in temperature but the self correcting feature of the relay would automatically adjust. If an alarm was only received once, the relay was reset and allowed to correct the problem. If no further alarms were received then the problem was considered corrected. If further alarms were received personnel were sent to correct the problem.

During the initial commissioning of the breaker it was found that the 1 msec tolerance could not be met. Problems in the breaker had resulted in excessive pre-arcing of the contacts to the resistor. This caused the contact closure to be unstable. The zero voltage relay alarm tolerance was found to be a good indicator of proper operation of the breaker. Breaker problems seemed to result in unstable closing times of the contacts.

Restrikes and Arrester Failures

During the first year of operation two 500kV arrester failures were experienced in the 500kV substation during opening of the capacitor bank. The first failure occurred during the initial testing of the capacitor bank breaker after modifications had been made to the closing resistor contacts. The second failure occurred during a normal opening operation of the capacitor bank.

During the first failure of the arrester, personnel in the substation observed the slow thermal failure of the arrester after the opening of the capacitor breaker. Figure 5 illustrates the fault recording record of the voltage and current waveforms on the phase where the failure occurred.

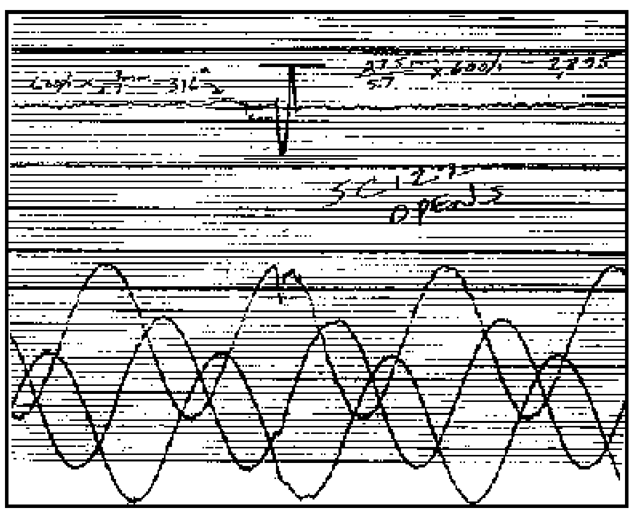

Figure 5 - Oscillograph Recording During Initial Arrester Failure

The top trace is the residual current in the neutral of the capacitor bank. The bottom three traces are the phase voltages. As can be seen from the trace the residual current was nearly zero until the 316 amp current begins which represents the opening of the first phase of the capacitor bank breaker. After a short delay the restrike inrush of 2895 amps is seen for one capacitor cycle and the event clears.

To help diagnose the problem, EMTP simulations were completed to evaluate opening the capacitor bank contacts in preset sequences until a close match of the measured and simulated neutral currents were obtained. The simulation result is illustrated in Figure 6.

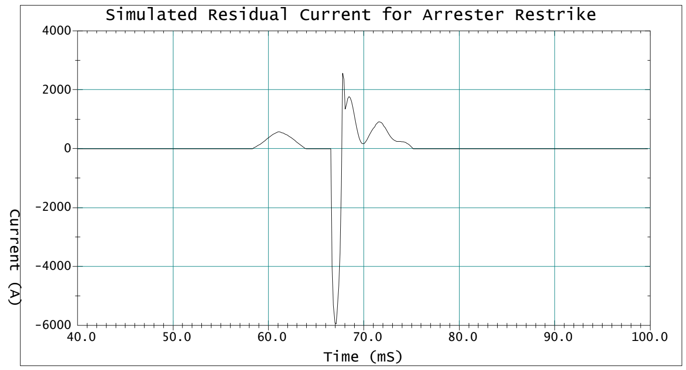

Figure 6 - EMTP Simulation of Arrester Restrike

A close correlation was found when phase A was interrupted first, phase C interrupted second, and phase B interrupted third. From the analysis it was decided that a restrike had occurred during contact opening near the voltage peak.

The original design used the philosophy that the MOV arresters at the capacitor bank would be able to protect the older silicon carbide arresters located on a transformer in the substation. The protective level of the MOVs were well below the protective level of the silicon carbide arresters. The manufacturer was contacted and agreed with the analysis that the MOV should protect the silicon carbide arresters. After the second restrike failure the remaining arresters were sent back to the factory for testing. It was found that the minimum breakdown voltage of the silicon carbide arresters were well below the protective level of the MOV arresters. This was thought to be a problem with the aging of the silicon carbide arrester. Since the minimum breakdown of the arrester is not a tested quantity, this was the only data on which to base the conclusions. It was decided that the aging of the silicon carbide arresters could produce lower levels of operation that would prevent the MOV arresters from protecting them during a capacitor breaker restrike. Because of this philosophy, using MOV arresters to protect silicon carbide arresters was stopped and the local substation arresters were changed to MOV arresters.

Yorktown 230kV Fuseless Capacitor Bank

Overview

Traditionally, the standard 230kV capacitor bank on the Virginia/North Carolina Power system is a fused 162 MVAr bank rated for operation up to 239kV. These banks consist of 540 - 300 kVAr units, each rated at 11.5kV. The banks are designed with 12 series groups per phase and 15 units per series group. Each capacitor can is individually fused with a 25 ampere T-link. Two separate frame structures per phase are required to house the 12 series groups.

The Yorktown fuseless capacitor bank was designed for 192 MVAr @ 249.4kV. The bank uses 480 - 400 kVAr units each rated at 7.2kV. There are eight parallel strings of capacitors per phase with 20 capacitor units per each string. The 20 units are connected in series with each other so that the sum of the individual unit voltages in the string will exceed the applied phase-to-ground voltage. The eight parallel strings per phase are needed to obtain the desired MVAr output. By not using fuses and flippers, and eliminating the space requirement between units for fuse operation, the 160 capacitor units per phase were mounted in a single frame structure per phase. It was estimated that the Yorktown bank used approximately one-third the volume of the traditional fused 230kV capacitor bank. Another advantage of the fuseless bank design is that no live parts are exposed. This reduces the banks vulnerability to animal damage and contamination.

Relay Protection Considerations

Considerations for capacitor unit overvoltage protection for a fuseless bank are essentially the same as those for a conventional fused bank. For the Yorktown fuseless capacitor bank, a voltage differential monitoring scheme was chosen. The voltage differential scheme consisted of a single meter accuracy CCVT per phase, connected to the 230kV bus, and a specially designed unbalance protection module connected between the capacitor bank rack and the neutral on each phase. The CCVT and protection module were connected to a microprocessor based voltage differential relay. The unbalance protection module used low-voltage capacitor units that were connected to an isolating potential transformer. Normal phase current from the capacitor bank develops a voltage across the low voltage capacitors which is then compared with the 230kV CCVT bus voltage. A capacitor unit failure will cause the phase current to increase, thus producing a differential voltage when compared with the 230kV bus CCVT voltage. Figure 7 illustrates the schematic diagram of the voltage differential scheme.

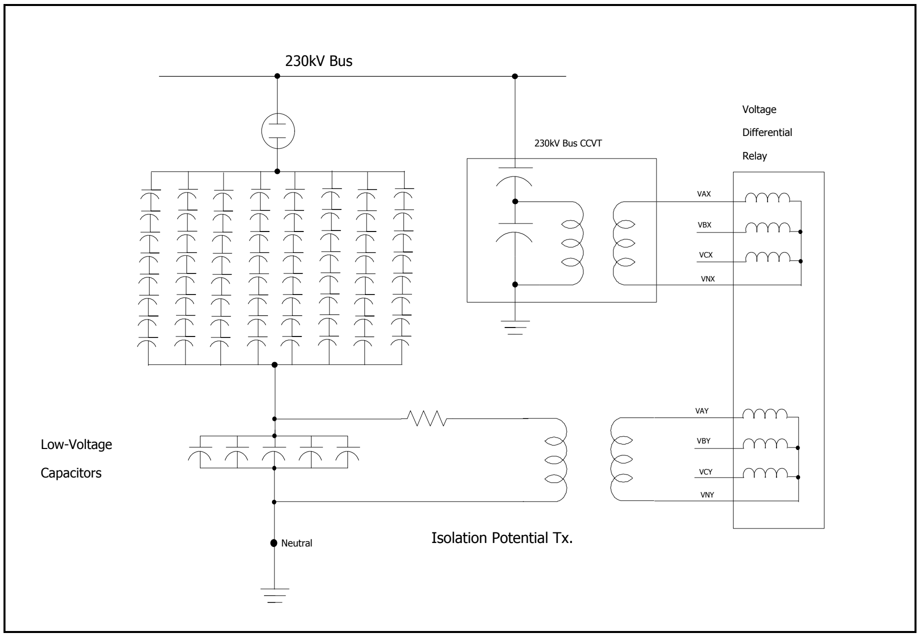

Figure 7 - Voltage Differential Protection Scheme

The unbalance protection module was designed because it was not economically feasible to install CCVTs at the midpoint of each of the eight capacitor strings. The protection module used five 167 kVAr capacitors per phase. The low-voltage capacitors were rated at 825 volts, 4 ohms, and were not fused. Five low-voltage capacitors per phase were chosen so that the voltage developed across each of the capacitors would not exceed 400 volts during normal bank operation. A 800/250 volt isolating potential transformer rated at 95kV BIL, was connected across the low-voltage capacitors. Any unbalance differential voltage that exists between the CCVT and the protection module during normal operation can be nulled out using the Ratio Adjustment feature in the voltage differential relay.

Failure of a single capacitor unit will cause the string overvoltage to increase by 5.3% while producing a 0.7% increase in the phase current. The voltage differential relay alarm unit was set to pickup for a single can failure and initiate the station annunciator alarm. The differential trip unit was set to detect failure of two capacitor units in a series string. The high set differential trip unit was set at twice the differential trip unit setting. Both the differential trip unit and the high-set unit are "masked" to trip the capacitor bank lockout relay and remove the bank from service.

Field Testing

A visual inspection of bank was done to check the installation for proper connections. Once this was completed, individual readings for each capacitor unit were performed. The capacitor test set used for fused capacitor banks was also used to perform the test for the fuseless capacitor bank. The test set consists of a variable 60 Hz voltage source with probes mounted to hotsticks for measurements from the ground level. The 60 Hz test voltage was applied to the de-energized bank through the phase leads. This applied the test voltage across an entire phase, causing current to flow through each of the capacitor units. The voltage drop across each capacitor unit was then measured and recorded along with the current in each string. These measurements were performed so that a defective unit could be quickly identified. Should a failure occur, the microprocessor relay would indicate which phase had the failure. The current in each string would then be measured to find which of the eight strings had the bad capacitor unit. The voltage across each unit in the string would then be measured until the defective unit was found.

Prior to installing the microprocessor based voltage differential relay on the panel, the relay response was tested using computer generated transient simulations. Twenty-four specially designed transient and/or steady state simulations were prepared. The simulations were specially prepared to present unusual conditions that the relay might be subjected to. Many of the simulated cases were conditions that caused the present neutral unbalance scheme to false operate.

A complete operational test of the entire voltage differential scheme was performed at the substation prior to the initial energizing of the bank. A laptop computer with two RS-232 serial ports was used to test the communications link and then download the new relay settings to the microprocessor relay. The computer was then used to simultaneously control the test sets and the relay for the operational test. Script files were prepared in advance to control the test sets which would apply the proper voltage inputs to the relay and simultaneously issue commands to the relay. Each individual element in the relay was tested for proper pickup via target lamp illumination and contact closure.

Following the initial energization, tests were made to check the voltage differential relay by externally shorting capacitor units. With the bank de-energized, an external short was connected across the bushings of one capacitor unit in one string on phase A. The bank was then energized to test the relay for a one unit out condition. The relay picked up, and after a three minute delay, the station annunciator alarm operated. The bank was then removed from service and the short was placed on the B and C phases, respectively. A second short, two units out, was also placed on each phase to test the differential tripping unit. In each case the relay picked up, operated the lockout relay, and correctly tripped the circuit switcher removing the bank from service. After completing these tests the bank was released for operation.

Operational History

Since the correction of the restrike problem on the 500kV capacitor bank at Morrisville the performance of the bank has been excellent. Both the zero voltage closing control and the opening performance has been perfect. The bank has been inservice daily for the summer heavy load period with no operational problems.

Since releasing the Yorktown fuseless bank in May 1992, the performance has been excellent. It has also been operated during heavy loads during the summer and winter without any problems. There have been no unit failures reported to date, which is a major improvement over the fused banks.

Conclusions

- The application of zero voltage closing control, in conjunction with a preinsertion resistor, has proven to be an effective method for controlling overvoltages associated with energizing the Morrisville 500kV capacitor bank.
- The use of the EMTP program as a tool to determine the mode of failure of the circuit breaker and arrester was extremely beneficial.
- The voltage differential relay protection scheme using a microprocessor based relay can be used to provide overvoltage protection where low sensitivity settings are needed. Meter accuracy or relay accuracy CCVTs can be used to provide voltage input to the differential scheme.
- The application of a fuseless capacitor bank, in a hostile environment for fuses, has been proven at 230kV with the additional benefit of reduced space.
- Low-voltage capacitors can be used as part of voltage differential scheme to provide accurate relay protection of a fuseless capacitor bank.

- Fuseless capacitor bank design and operation can be accomplished without any change to the existing relay protection and operating philosophies.

References

[1] P.W. Powell, J.F. Peggs, “230kV Capacitor Bank Protection,” *Georgia Tech Protective Relay Conference, 1991.*

[2] J.E. Harder, “Fuseless Substation Capacitor Banks,” *Pennsylvania Electric Association Conference, 1990.*

[3] R. W. Flugum and J. W. Kalb, “Operation of Surge Arresters on Low Surge Impedance Circuits,” Presented at the *IEEE PES Winter Meeting* January 27-February 1, 1974, New York.

[4] S. S. Mikhail and M. F. McGranaghan, “Evaluation of Switching Concerns Associated with 345kV Shunt Capacitor Applications,” *IEEE Transactions on Power Systems*, Vol. PWRD-1, No. 2, April 1986.

Jeff Peggs and Phillip Powell, Virginia Power
Thomas Grebe, Electrotek Concepts, Inc.

Ungrounded System Analysis

Transient Analysis of a Three-Phase Ungrounded Primary Distribution System

Introduction

Ungrounded primary distribution systems (delta connected) are used to provide a higher degree of reliability than do grounded systems. This is because the ungrounded system can, in principle, tolerate a single-line-to-ground (SLG) fault without loss of load. However, a SLG fault on an ungrounded system may initiate transient overvoltages on the unfaulted phases. These overvoltages have been known to result in a ground fault on an unfaulted phase. This results in breaker operation, removing the feeder from service due to the line-line-to-ground fault. Consequently the assumed higher degree of reliability of the ungrounded system may not be realized.

The project discussed in this article involved the transient analyses of a three-phase, delta connected, ungrounded distribution system, with a line-to-line voltage of 4,160 volts. System load is approximately 1 mVA. The principal concerns of the analyses were transient voltage on the unfaulted phases resulting from a SLG fault. The analysis was carried out using a three-phase EMTP simulation. The simulation utilized EMTP models of cable, transformers, load and switches. The EMTP simulation of ungrounded systems is of particular interest. While straightforward, it is somewhat unusual. The simulation provided the phase voltage responses due to SLG faults. These were used in subsequent studies.

Description of the Problem

Three-phase primary distribution systems are often operated ungrounded as a means of avoiding outages at critical times. The ungrounded system can tolerate a line to ground fault without an interruption. However it is always necessary to detect such a fault and to clear it in an appropriate time. It should be pointed out that the ungrounded system is in fact capacitively coupled to ground. When we speak of an ungrounded system we actually mean a system which is not intentionally grounded as shown in Figure 1.

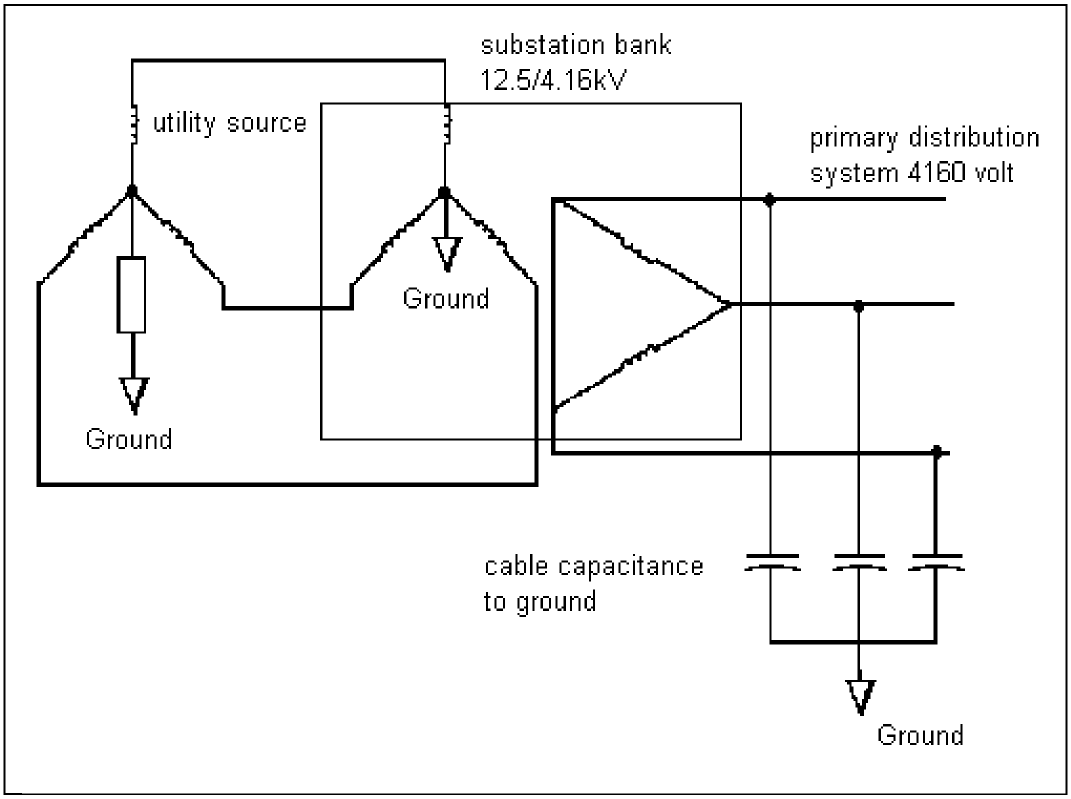

Figure 1 - Ungrounded Primary Distribution System Showing Source and Cable Capacitance to Ground

A single line diagram from the substation bank is shown in Figure 2.

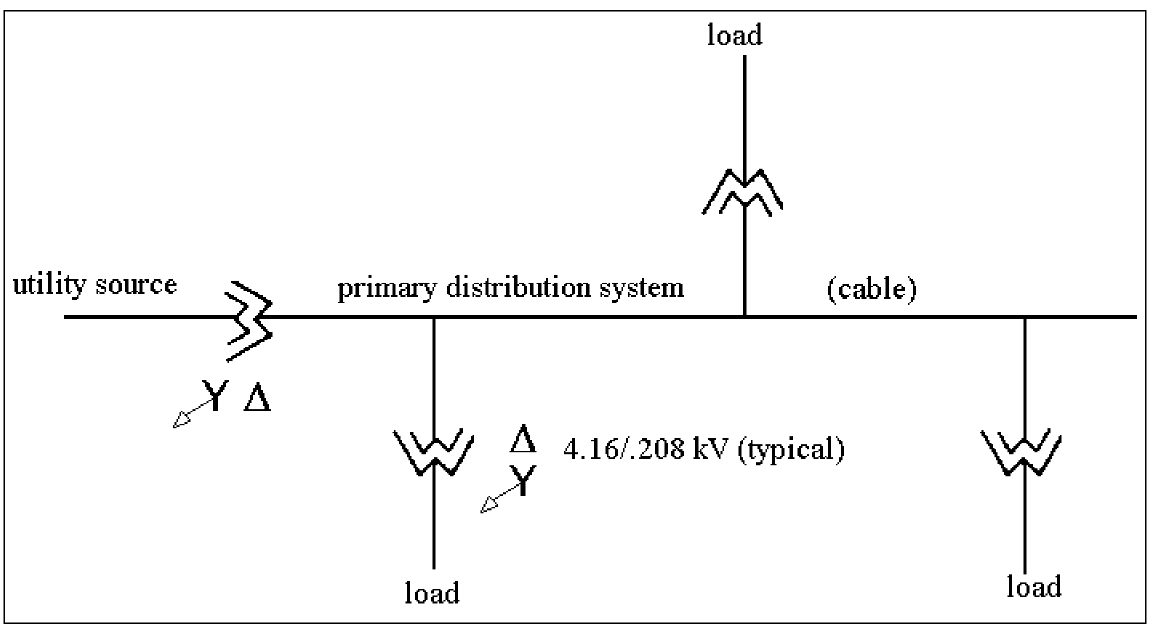

Figure 2 - Single Line Diagram

Note that the loads are connected to the primary distribution system by Δ Y transformers, leaving the primary system ungrounded. Because of their cable capacitive coupling, the normal line to ground in the primary system is

$$\frac{4160}{\sqrt{3}} \text{ volts rms.}$$

In the event of a line-to-ground fault, the steady-state voltage on the ungrounded phases is 4160 volts rms. Cable and transformer insulation must tolerate this increase in steady-state line-to-ground voltage. However, the transient line-to-ground voltages initiated by a line-to-ground fault may substantially exceed the steady-state voltages.

Transient overvoltages, initiated by a fault, are due to excitation resonances involving the inductances and capacitances of the primary distribution system. To study these overvoltages an EMTP simulation of the system was developed. The simulation included the utility source, substation bank, distribution cable, load transformers and loads in a three phase representation. An additional component which was simulated was a three-phase grounding bank, as shown in Figure 3.

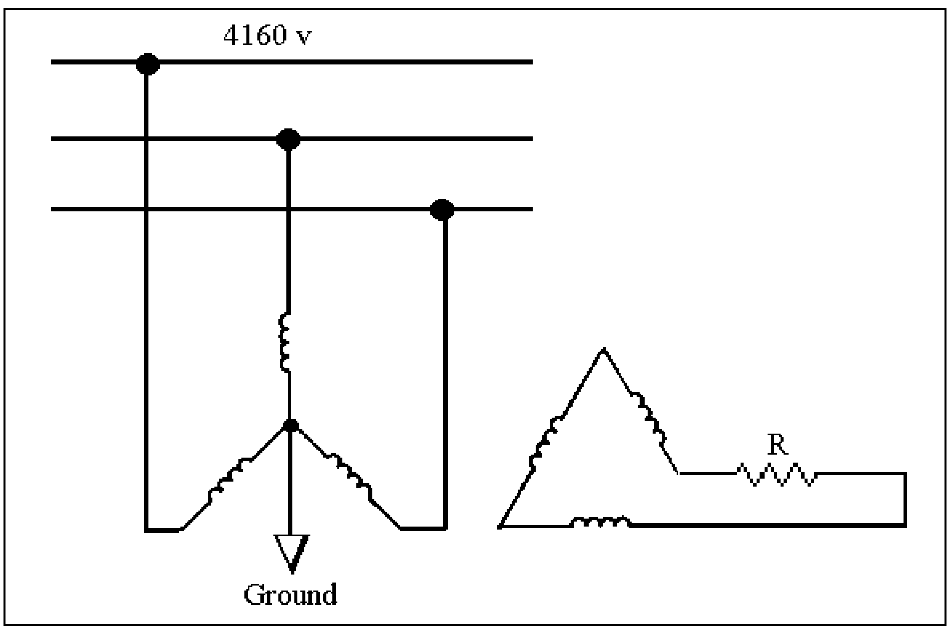

Figure 3 - Grounding Bank

Analysis of EMTP Simulation Results

The grounding bank is a grounded Y primary/open Δ secondary, with the secondary closed through a resistor R Ω. The grounding bank carries only excitation current under unfaulted conditions. Current through R is an indication of a line-to-ground fault on the primary distribution system. The EMTP simulation was used to study transient voltages on the unfaulted phases, fault current and current through R for cases of solid (25 Ω) line-to-ground faults as well as arcing line-to-ground faults.

Some typical simulation results are shown in Figures 4 through 7. We see that the transient voltage to ground on an unfaulted phase rises to about 7000 volts, about 2.06 per unit of the normal phase to ground voltage. Some high frequency ringing occurs as seen in Figure 5, showing the primary fault current. The secondary current in the grounding bank (through R) rises to its steady-state value almost immediately as seen in Figure 6. Figure 7 shows phase voltages for the case of an arcing fault on phase A, the arc being initiated as a phase to ground voltage of 2000 volts.

SLG Fault on Phase A

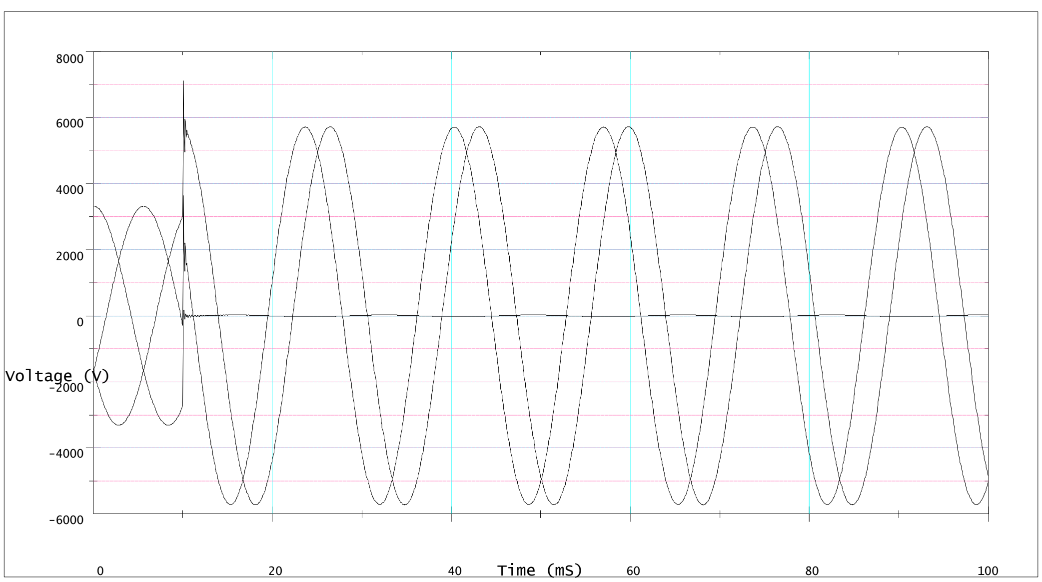

Figure 4 - Phase Voltages to Ground

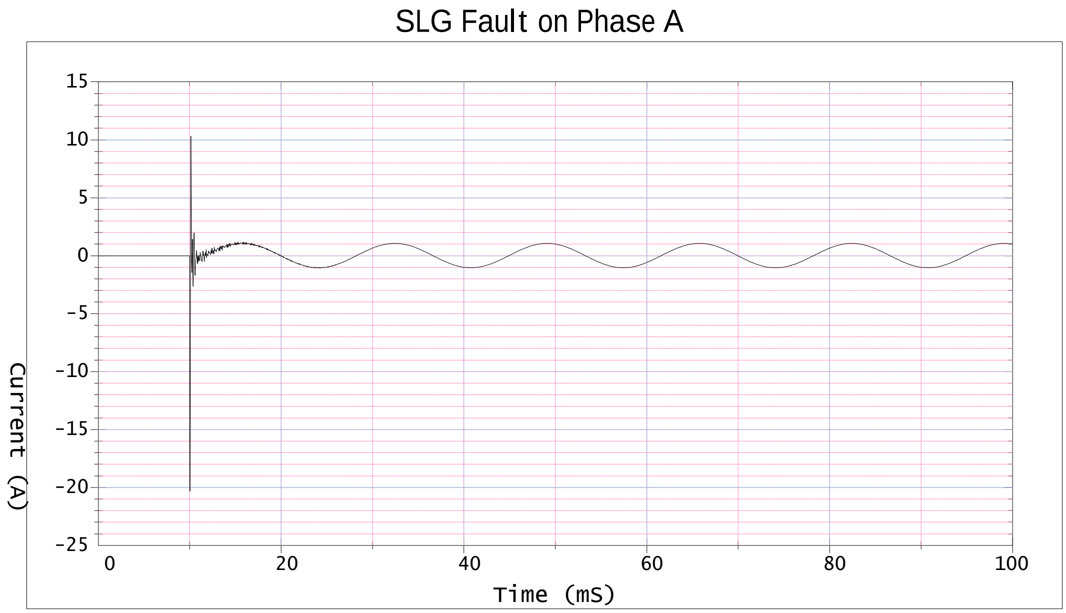

Figure 5 - Fault Current Phase A to Ground

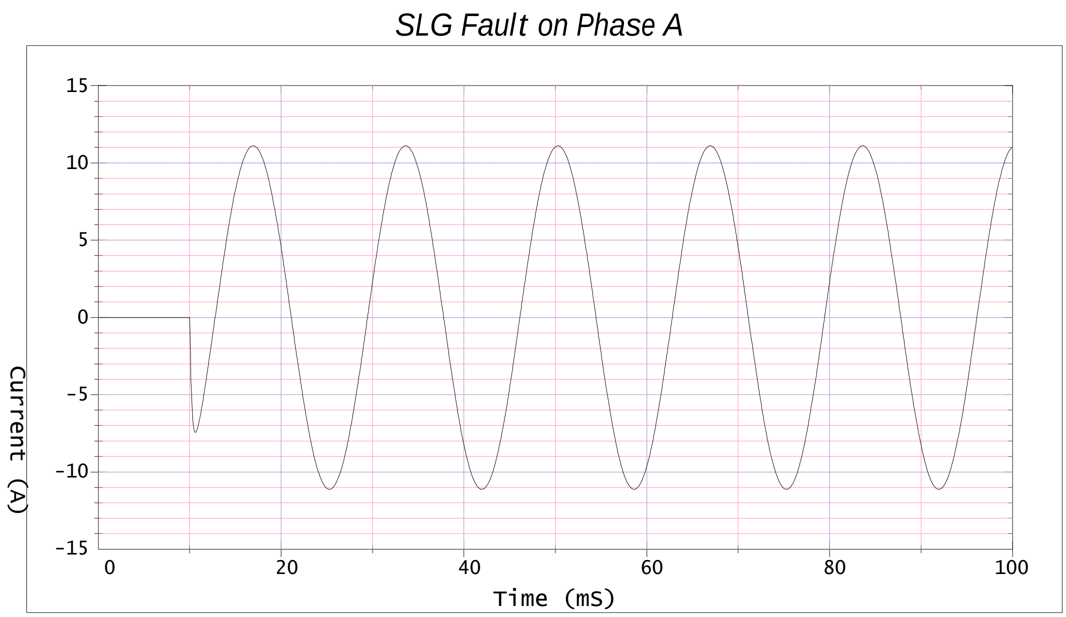

Figure 6 - Secondary Current in Grounding Bank

SLG Fault on Phase A

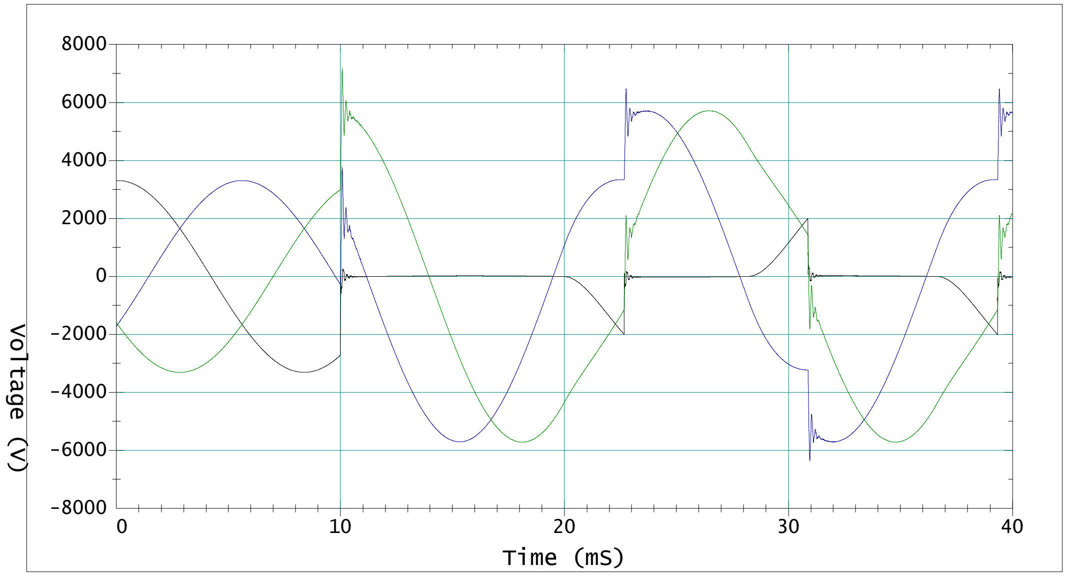

Figure 7 - Phase Voltages to Ground

It was determined that a small arc resistance, approximately 25 Ω, had to be used in the EMTP simulation to prevent excessive numerical oscillation. Based on previous experience with this type of oscillation, this did not seem to be an unreasonable value.

The ungrounded voltage source required in this EMTP simulation was accomplished using the Type 18 source and carefully following the instructions given in the Rule Book. The arcing fault was modeled in part using a Class 2 flashover switch.

William F. Horton, Professor
Saul Goldberg, Professor and Chariman
Cal Poly State Univeristy
San Luis Obispo, CA